Antiproton Anomalies in Space: Hadronic Cross Sections and Uncertainties in Cosmic Ray Physics

Jennifer Rittenhouse West
INFN Section Turin & University of Turin

XX Conference on Theoretical Nuclear Physics in Italy
Cortona, Il Palazzone, Italia
1-3 October 2025



Istituto Nazionale di Fisica Nucleare

SEZIONE DI TORINO



Diquarks in Nuclei: Quark-Quark bonds as the elementary QCD basis for Short-range correlations & an alternative to Gluon Junctions

Jennifer Rittenhouse West INFN Section Turin & University of Turin

XX Conference on Theoretical Nuclear Physics in Italy Cortona, Il Palazzone, Italia 1-3 October 2025



Istituto Nazionale di Fisica Nucleare

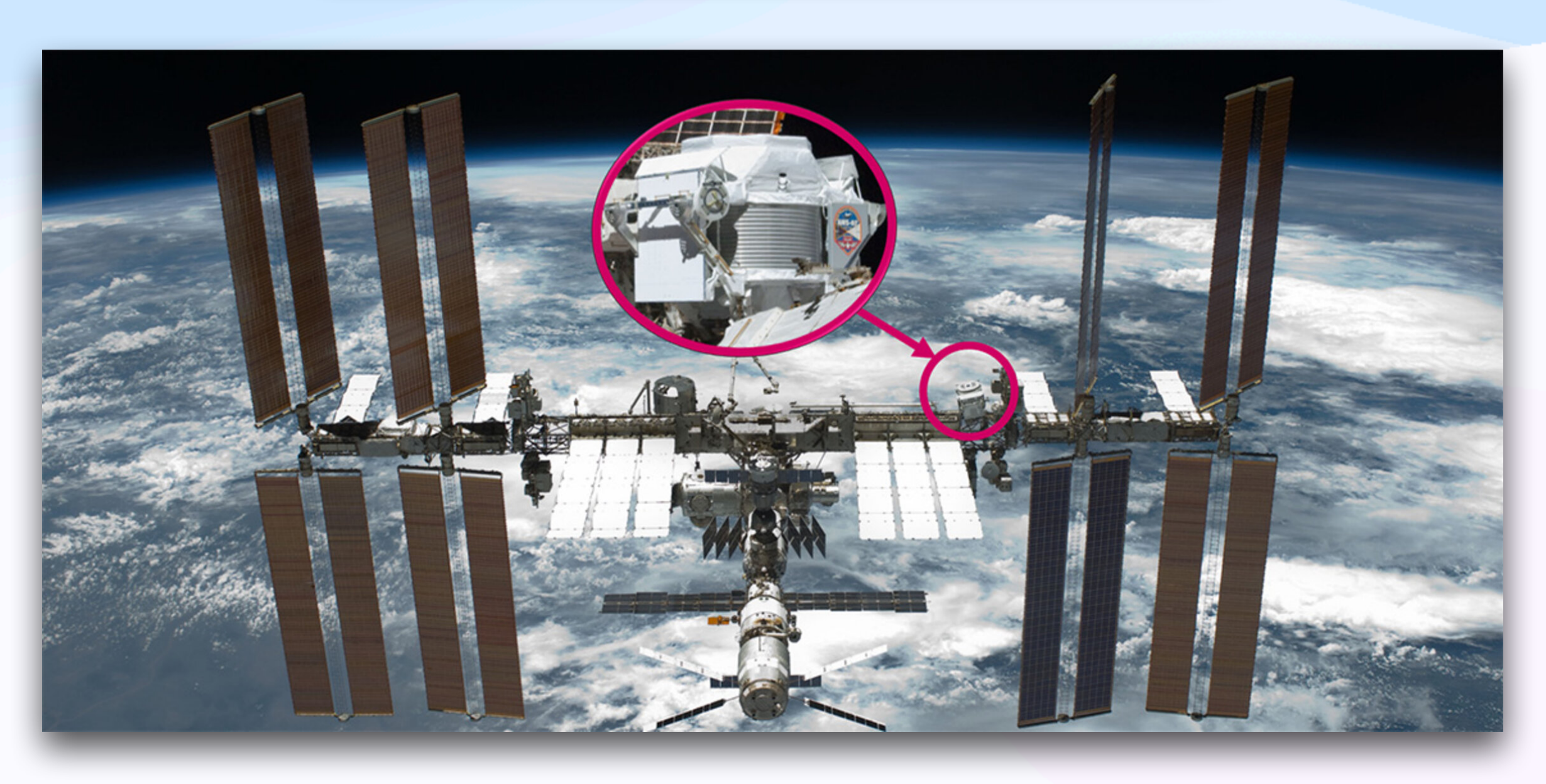




Antiparticle detector in space, AMS-02

- AMS-02 particle detector, assembled at CERN
- Launched to the ISS 2011
- PI Sam Ting, 1976 Nobel prize with Burt Richter for J/ψ
- Searching for: dark matter annihilation, dark matter decays
- Detectors for: protons, antiprotons, positrons, light nuclei and antinuclei
- Antiprotons: High energy cosmic ray collisions with interstellar gas





Alpha Magnetic Spectrometer (AMS-02) on the International Space Station, image credits NASA via ESA

Antiproton Creation in Cosmic Rays

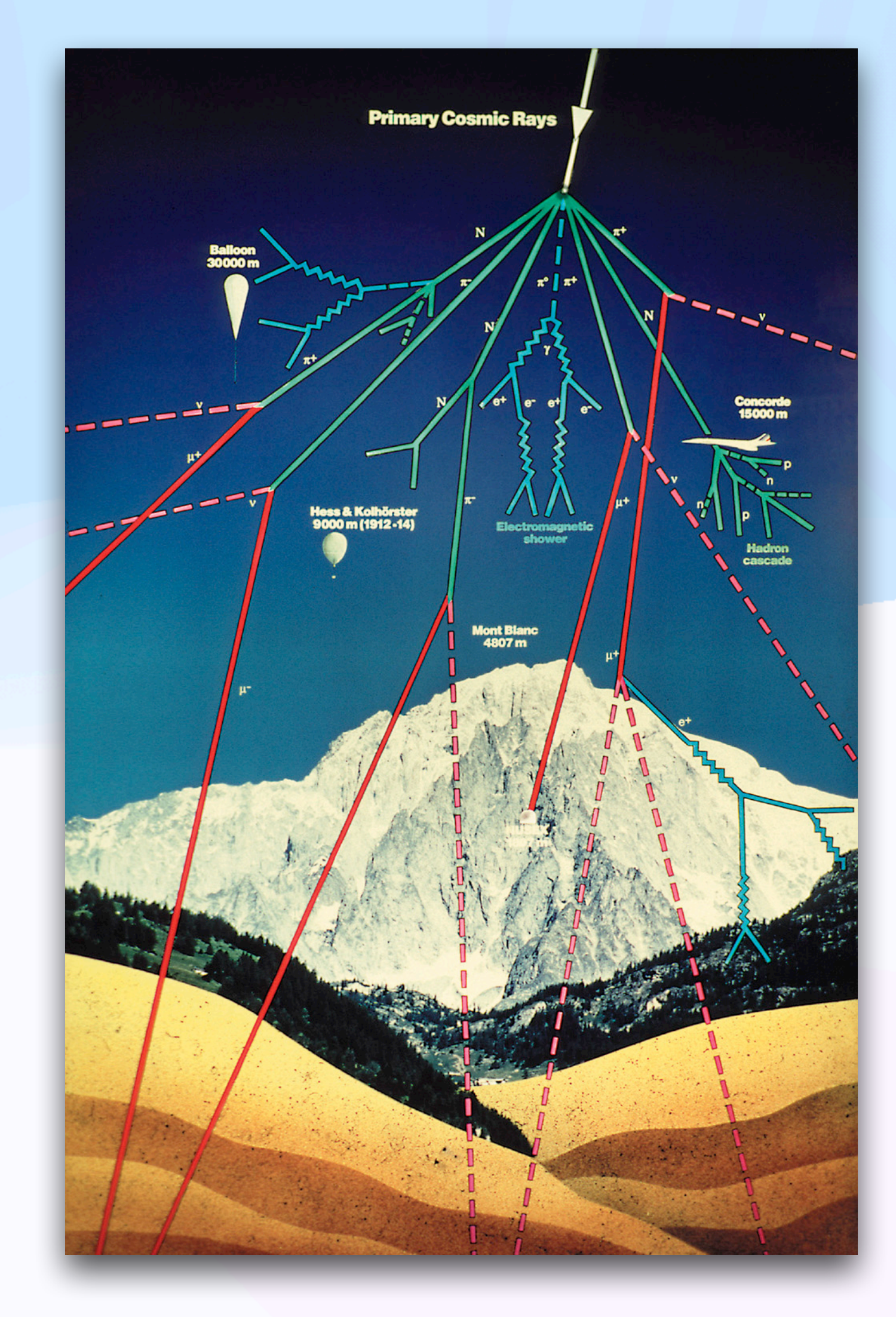
Classification of cosmic rays:

- 1. **PRIMARY COSMIC RAYS**: Particles accelerated at astrophysical sources (e.g., produced by supernovae mostly protons aka H)
- 2. **SECONDARY COSMIC RAYS**: Particles produced in interaction of the primaries with interstellar gas (i.e., H, ²He, plus traces)

Antiprotons are **SECONDARIES**, produced directly in $p+p \to \bar{p}$ and indirectly in $p+p \to \bar{n}$ (with $\bar{n} \to \bar{p} + e^+ + \nu_e$, branching ratio 1).

Astrophysics model "naive" assumption circa ~2014:

By isospin symmetry, $N_{\bar{p}}=N_{\bar{n}}$. .: to find $N_{\bar{n}}$, multiply expected antiproton abundance by 2.



Antiprotons Observed by AMS-02

A Robust Excess in the Cosmic-Ray Antiproton Spectrum: Implications for Annihilating Dark Matter

Ilias Cholis (Oakland U.), Tim Linden (Ohio State U.), Dan Hooper (Chicago U., Astron. Astrophys. Ctr. and Fermilab) Mar 6, 2019

Published in: Phys.Rev.D 99 (2019) 10, 103026

Published: May 31, 2019

e-Print: 1903.02549 [astro-ph.HE] DOI: 10.1103/PhysRevD.99.103026

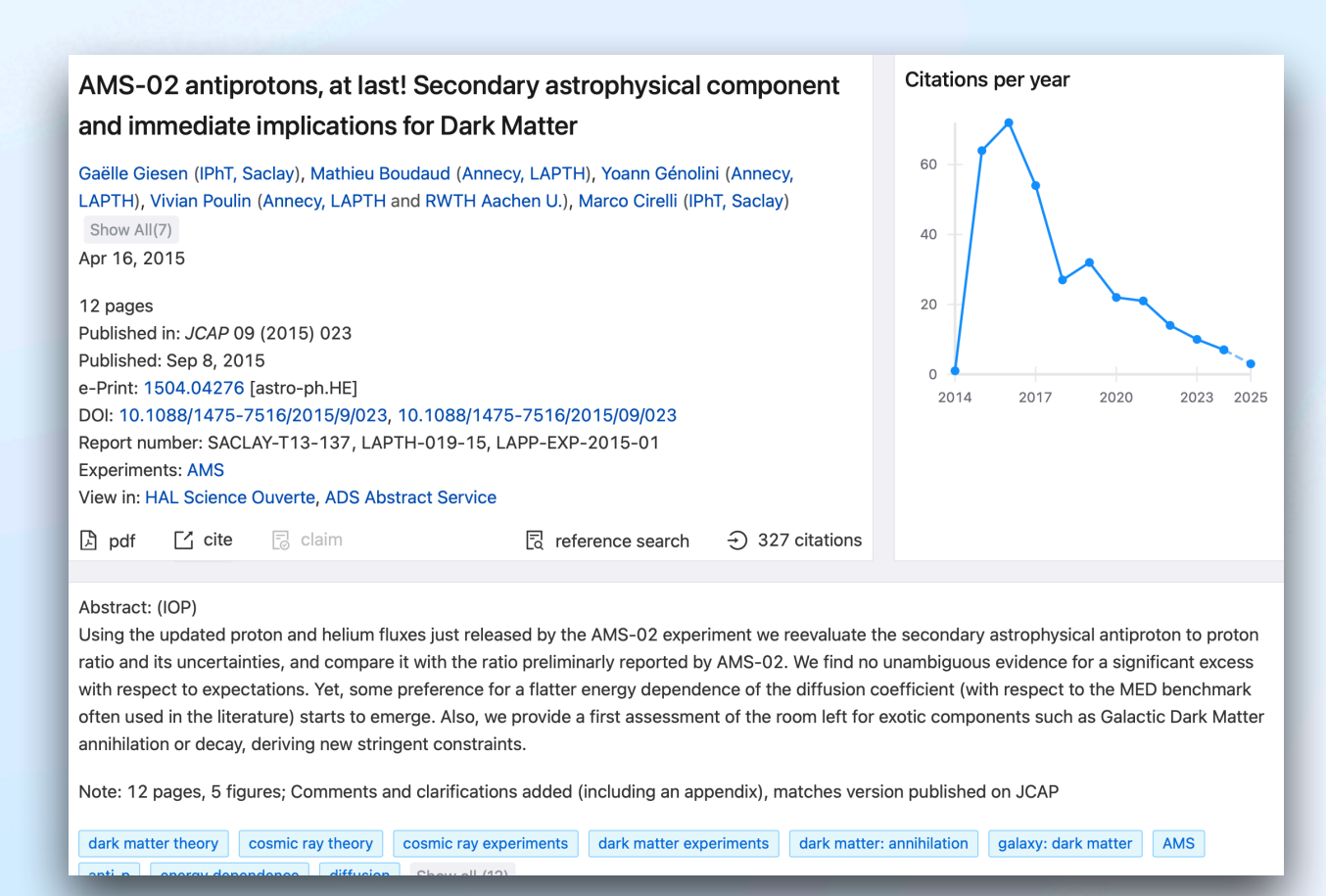
Report number: FERMILAB-PUB-19-091-A



An excess of ~10–20 GeV cosmic-ray antiprotons has been identified in the spectrum reported by the AMS-02 Collaboration. The systematic uncertainties associated with this signal, however, have made it difficult to interpret these results. In this paper, we revisit the uncertainties associated with the time, charge and energy-dependent effects of solar modulation, the antiproton production cross section, and interstellar cosmic-ray propagation. After accounting for these uncertainties, we confirm the presence of a 4.7σ antiproton excess, consistent with that arising from a mx≈64–88 GeV dark matter particle annihilating to bb with a cross section of σv≈(0.8–5.2)×10-26 cm3/s. If we allow for the stochastic acceleration of secondary antiprotons in supernova remnants, the data continue to favor a similar range of dark matter models (mx≈46–94 GeV, σv≈(0.7–3.8)×10-26 cm3/s) with a significance of 3.3σ. The same range of dark matter models that are favored to explain the antiproton excess can also accommodate the excess of GeV-scale gamma rays observed from the

Citations per year

Excess exists! Uncertainties are large but we find 4.7σ evidence.



Excess does not exist!

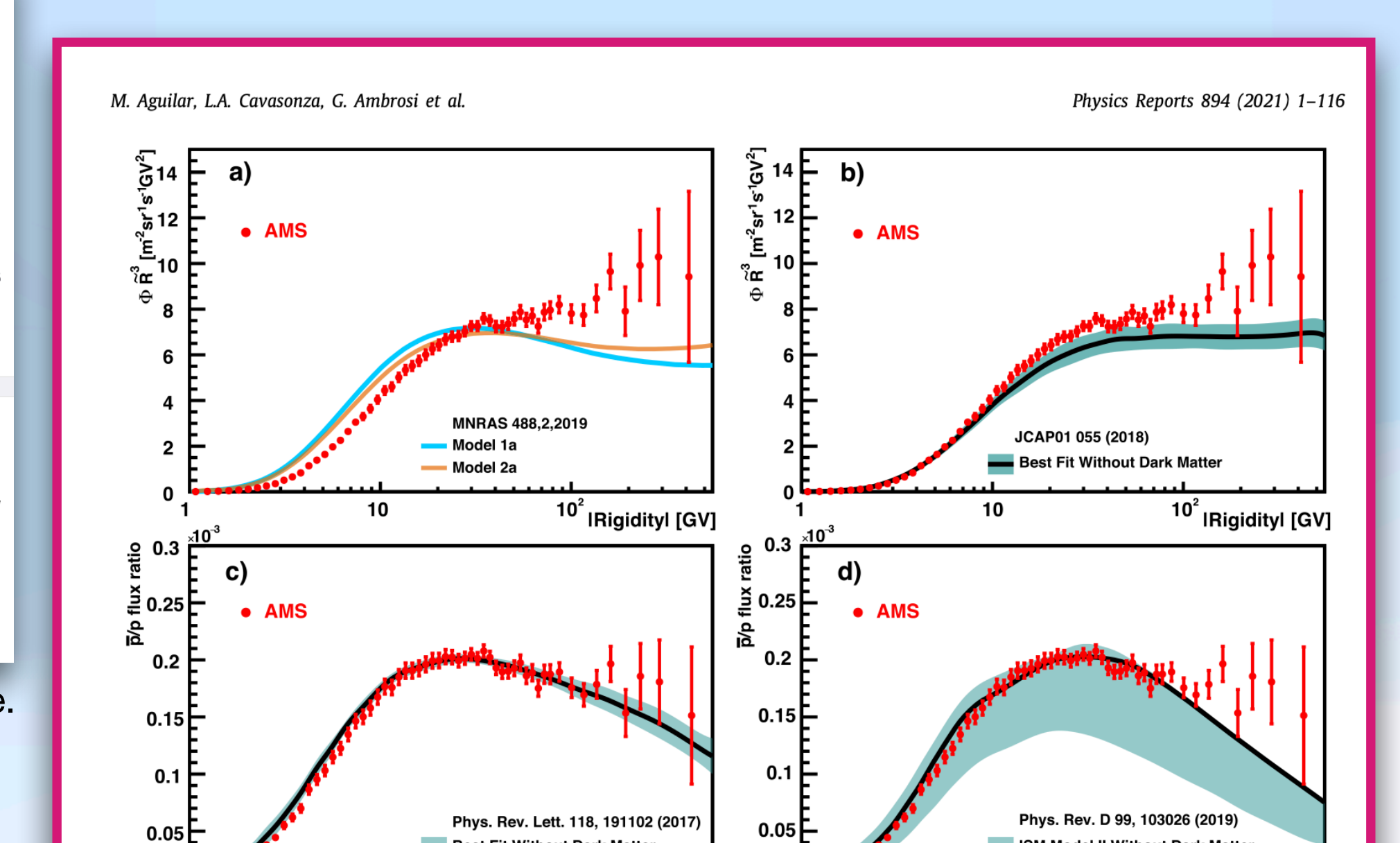


Fig. 62. (a), (b) The AMS antiproton spectrum and (c), (d) the antiproton-to-proton flux ratio (red data points) together with five recent theoretical models that include only collisions of cosmic rays (solid lines) [113,114]. In (a) the orange and blue solid lines show the same model predictions with two different sets of model assumptions. The uncertainties of the models in (b), (c) and (d) are indicated as blue bands.

ISM Model II Without Dark Matte

"The Alpha Magnetic Spectrometer (AMS) on the International Space Station: Part II— Results from the first seven years" 2021

(Rigidity:
$$R = \frac{pc}{Ze}$$
)

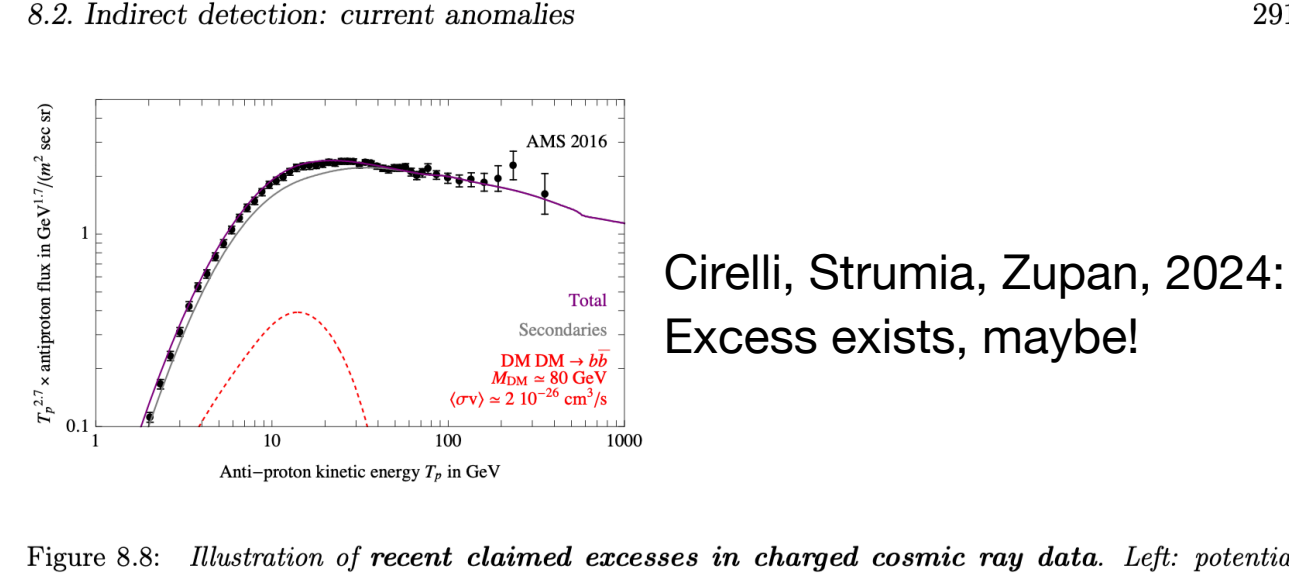
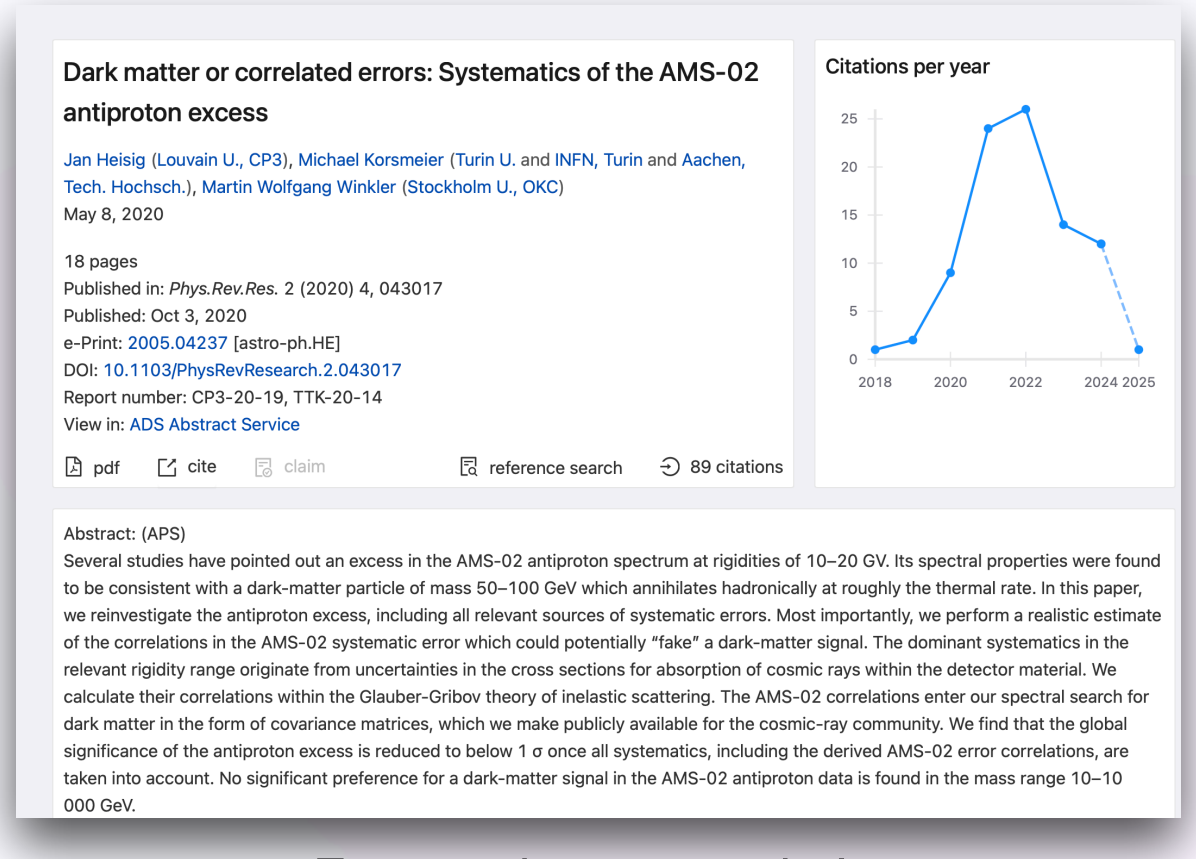


Figure 8.8: Illustration of recent claimed excesses in charged cosmic ray data. Left: potential antiproton excess in AMS data. The grey line represents the astrophysical flux of secondary \bar{p} that, together with a DM contribution (red dashed line), would best fits the data according to recent studies. The secondary \bar{p} best fit flux without DM is not shown. Right: possible lepton excess in DAMPE data.

Antiprotons in Space: Some evidence for anomalous spectral behavior. Possible excess of antiprotons. Hadronic cross section calculations needed.



Excess does not exist!

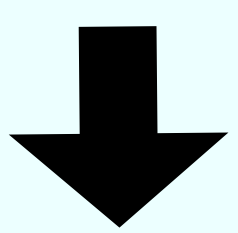
Antiprotons Observed with Possible Anomalies, however...

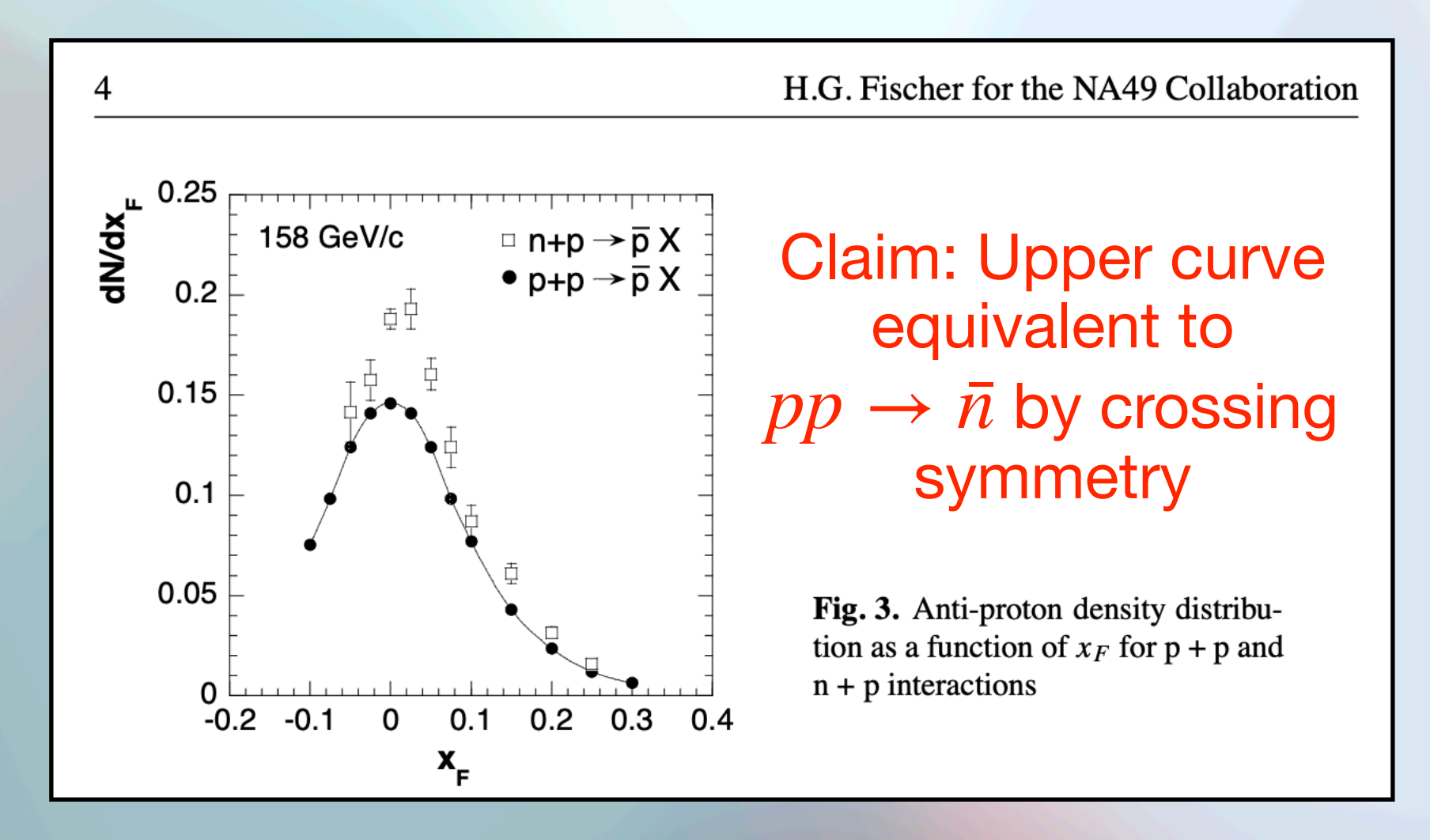
For the production processes we need the cross sections $\sigma_{pH\to\bar{p}X}$, $\sigma_{pHe\to\bar{p}X}$, $\sigma_{\alpha H\to\bar{p}X}$, $\sigma_{\alpha H\to\bar{p}X}$, where the first index refers to the impingent primary CR while the second one to the target interstellar material. For σ_{pH} we use the new parameterization recently proposed by [44], instead of the traditional fitting relations given in [48, 49]. For the cross sections of the other reactions we use the prescription of [40], to which we refer the interested reader. We just remind that for the cross section values that we adopt the pH reaction dominates, providing 60% to 65%of the total \bar{p} flux depending on the energy, while pHe and α H reactions yield 32 to 37%, and the reaction α He contributes less than 3%. Another element which has only recently been appreciated is related to the contribution of antineutron production: on the basis of isospin symmetry, one would consider the production cross section for antineutrons (e.g. $\sigma_{pH\to\bar{n}X}$ and the others) as equal to those for antiprotons; the antineutrons then rapidly decay and provide an exact factor of 2 in the \bar{p} flux. However, as pointed out in [44, 50] and as already implemented in [21], it may be that this naïve scaling does not apply and that the antineutron cross section is larger by up to 50% with respect to the \bar{p} one. Assessing uncertainties for reactions involving He is even more challenging, since no data are present, and predictions are based on semi-empirical nuclear models calibrated on data involving either protons or heavier nuclei (see [51]). For sure, uncertainties involving these reactions are at least as large in percentage as the one of the pH reaction, an assumption we will do in the following. More conservative assumptions would only make the error larger, and strengthen our main conclusion on the level of agreement of the data with a purely secondary antiproton flux. All these cumulated effects contribute to an uncertainty band for the astrophysical \bar{p}/p ratio which is represented in fig. 8 of [44] and which we will adopt: it varies from about 20% to at most 50% (at large energies and in the most conservative conditions). In fig. 1, top right panel, we show our prediction for the \bar{p}/p ratio with this uncertainty envelope.

[44] M. di Mauro, F. Donato, A. Goudelis and P. D. Serpico, Phys. Rev. D 90 (2014) 8, 085017 arXiv:1408.0288 [hep-ph].

[50] R. Kappl and M. W. Winkler, JCAP 1409 (2014) 051 [arXiv:1408.0299 [hep-ph]].

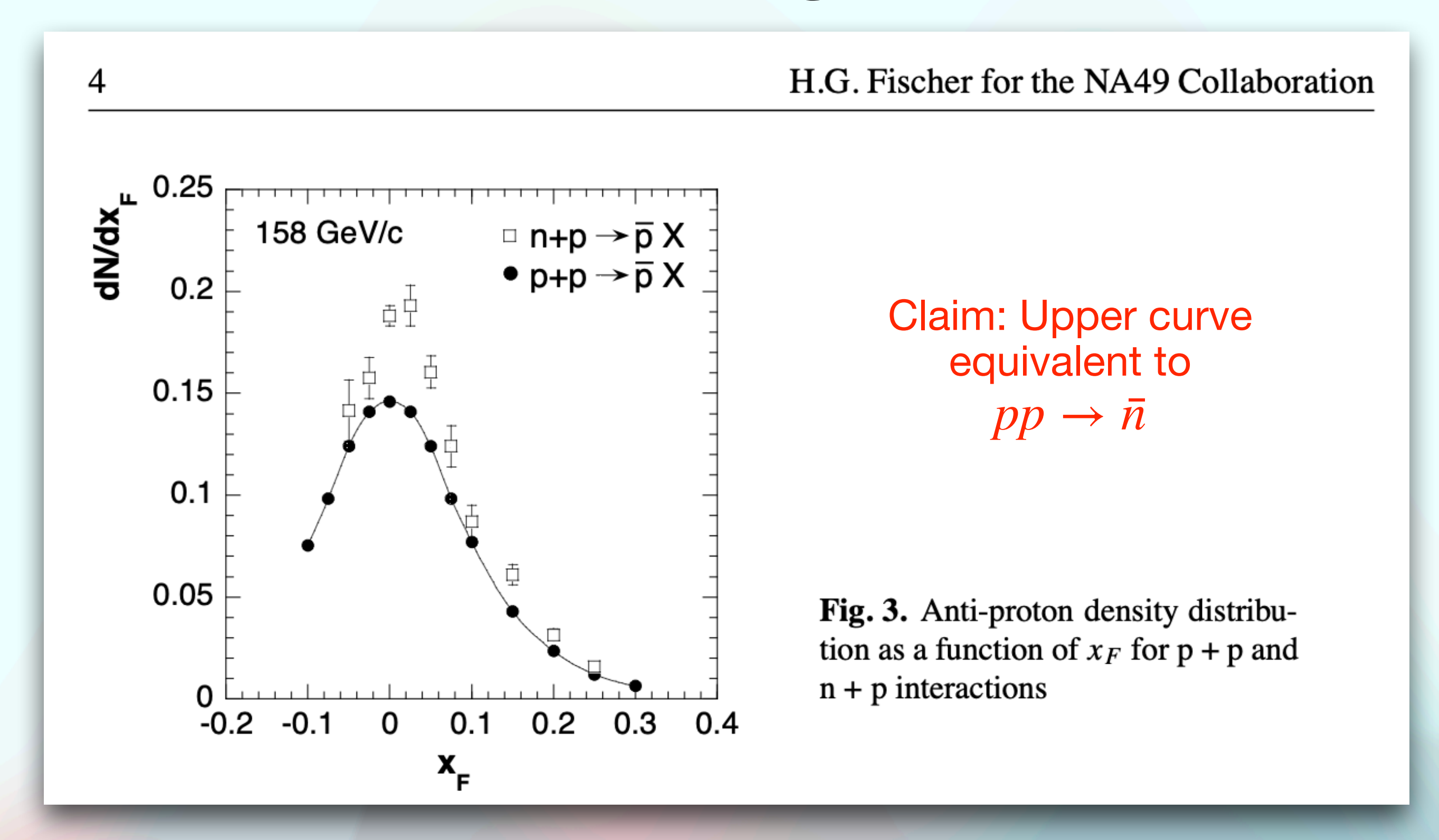
[21] M. Boudaud, M. Cirelli, G. Giesen and P. Salati, arXiv:1412.5696 [astro-ph.HE].





Needed: Cross section calculations from hadronic side with uncertainties!

NA49 Data used as possible evidence for Dark Matter signatures



Assumption in dark matter theory papers:

Crossing symmetry equates np o ar p to pp o ar n , \Longrightarrow indirect production ~33% higher than direct production

This introduces two possible errors:

Crossing symmetry applies at amplitude level. Partonic cross sections will differ from hadronic cross sections.

Antiproton pp $\rightarrow \bar{p}$, pp $\rightarrow \bar{n}$ cross section calculations

Running older (newly modified) Fortran code:

Factorized single-inclusive NLO cross section, $a+b\to c+X$ (unpolarized, $pp\to \bar{p}$ or other final state baryon):

$$E_{\bar{B}} \frac{d\sigma}{d^{3}p_{\bar{B}}} = \frac{1}{\pi S} \sum_{a,b,c} \int_{z_{0}}^{1} \frac{dz_{c}}{z_{c}^{2}} \int_{VW/z_{c}}^{1-(1-V)/z_{c}} \frac{dv}{v(1-v)} \int_{VW/vz_{c}}^{1} \frac{dw}{w} f_{a}(x_{a}, \mu_{F}) f_{b}(x_{b}, \mu_{F}) D_{c}^{\bar{B}}(z_{c}, \mu_{F}')$$

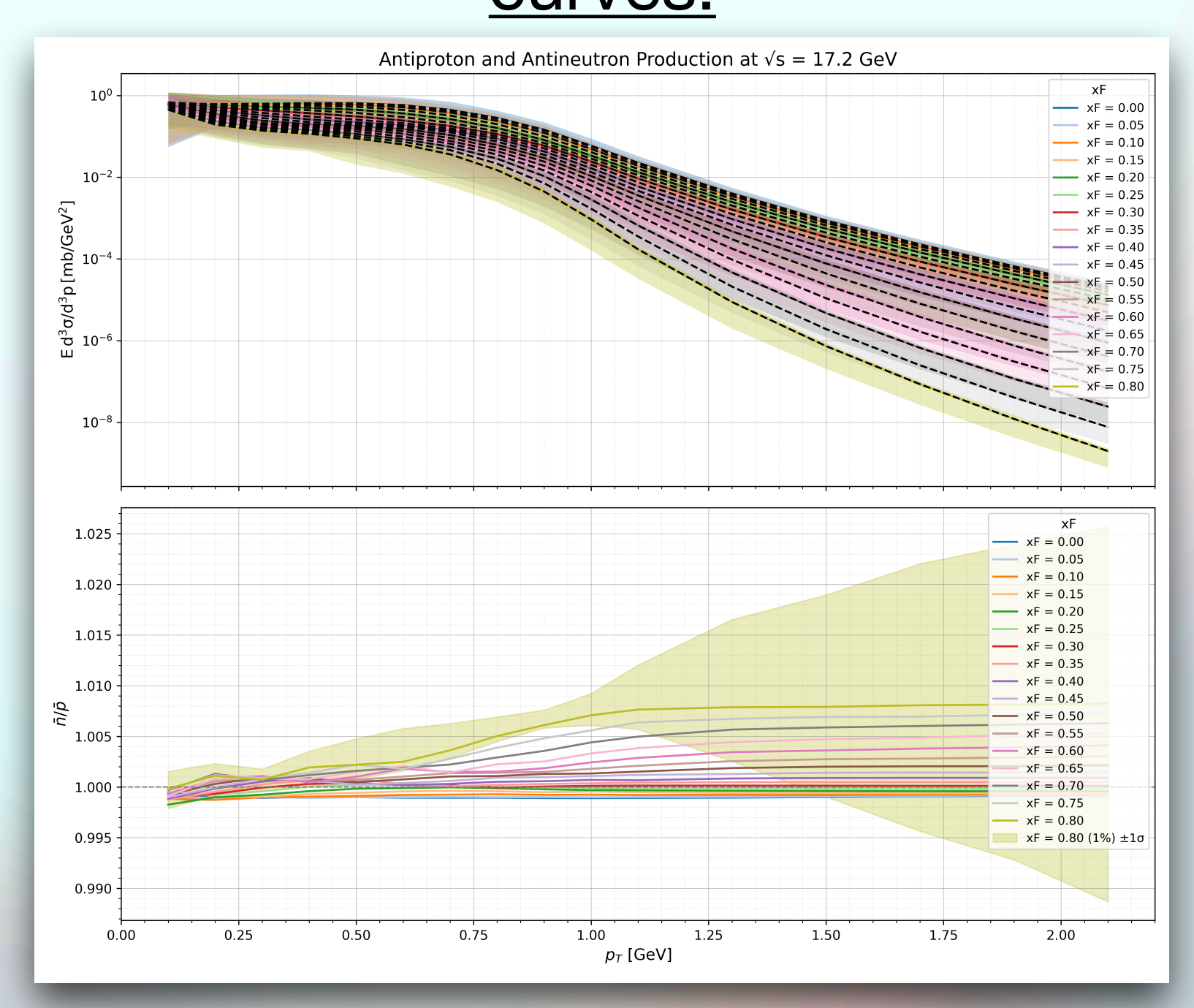
$$\times \left[\frac{d\hat{\sigma}_{ab}^{c,(0)}(v)}{dv} \delta(1-w) + \frac{\alpha_{s}(\mu_{R})}{\pi} \frac{d\hat{\sigma}_{ab}^{c,(1)}(s, v, w, \mu_{R}, \mu_{F}, \mu_{F}')}{dvdw} \right]$$

where
$$z_0 = 1 - V + VW$$
, with hadron level variables: $V \equiv 1 + \frac{T}{S}$, $W \equiv \frac{-U}{S+T}$, $S \equiv \left(P_A + P_B\right)^2$, $T \equiv \left(P_A - P_\pi\right)^2$, $U \equiv \left(P_B - P_\pi\right)^2$

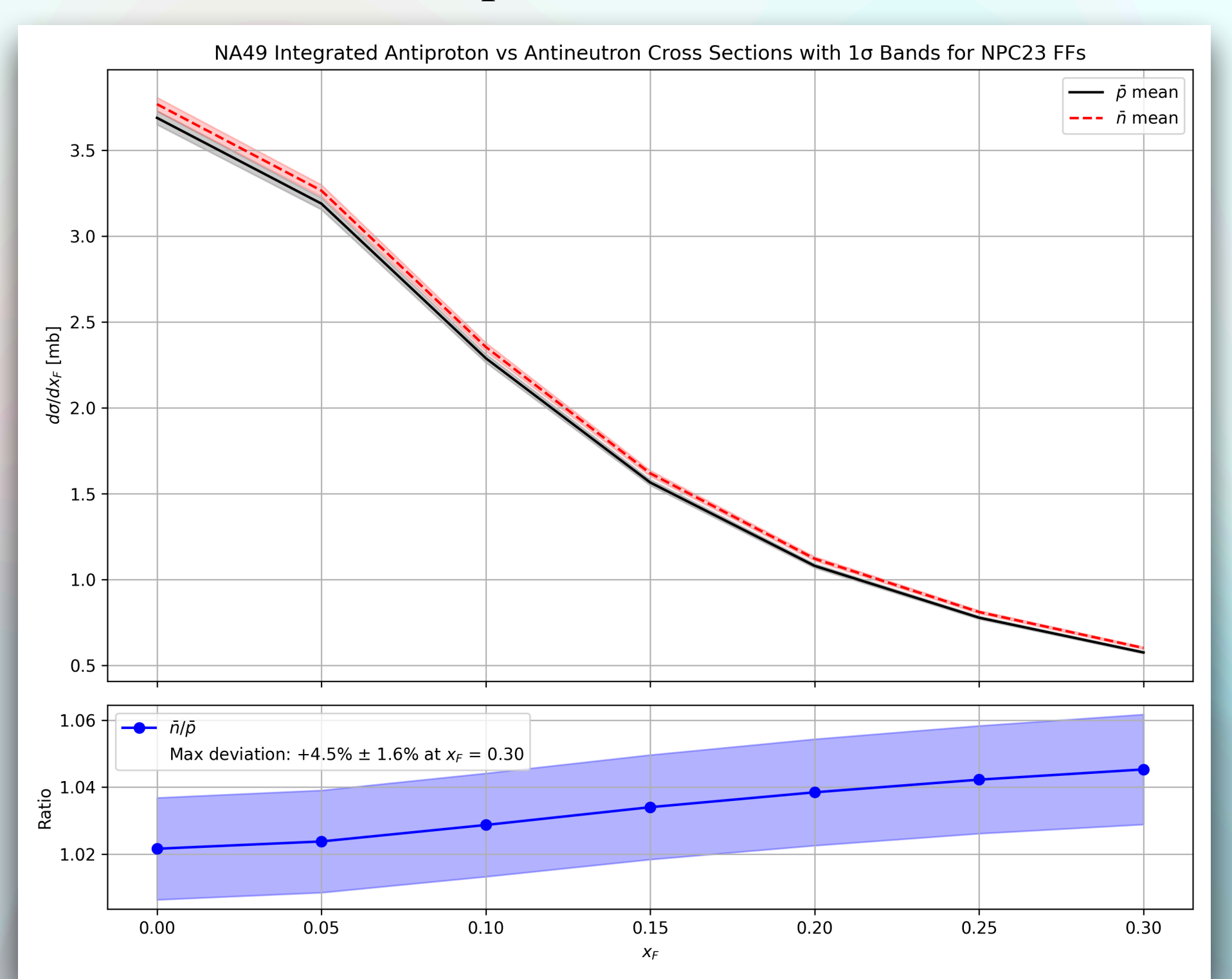
and corresponding partonic level variables:
$$v \equiv 1 + \frac{t}{s}$$
, $w \equiv \frac{-u}{s+t}$, $s \equiv (p_a + p_b)^2$, $t \equiv (p_a - p_c)^2$, $u \equiv (p_b - p_c)^2$

NA49 2010 Data vs. QCD/Pheno: $pp o \bar{n}, pp o \bar{p}$

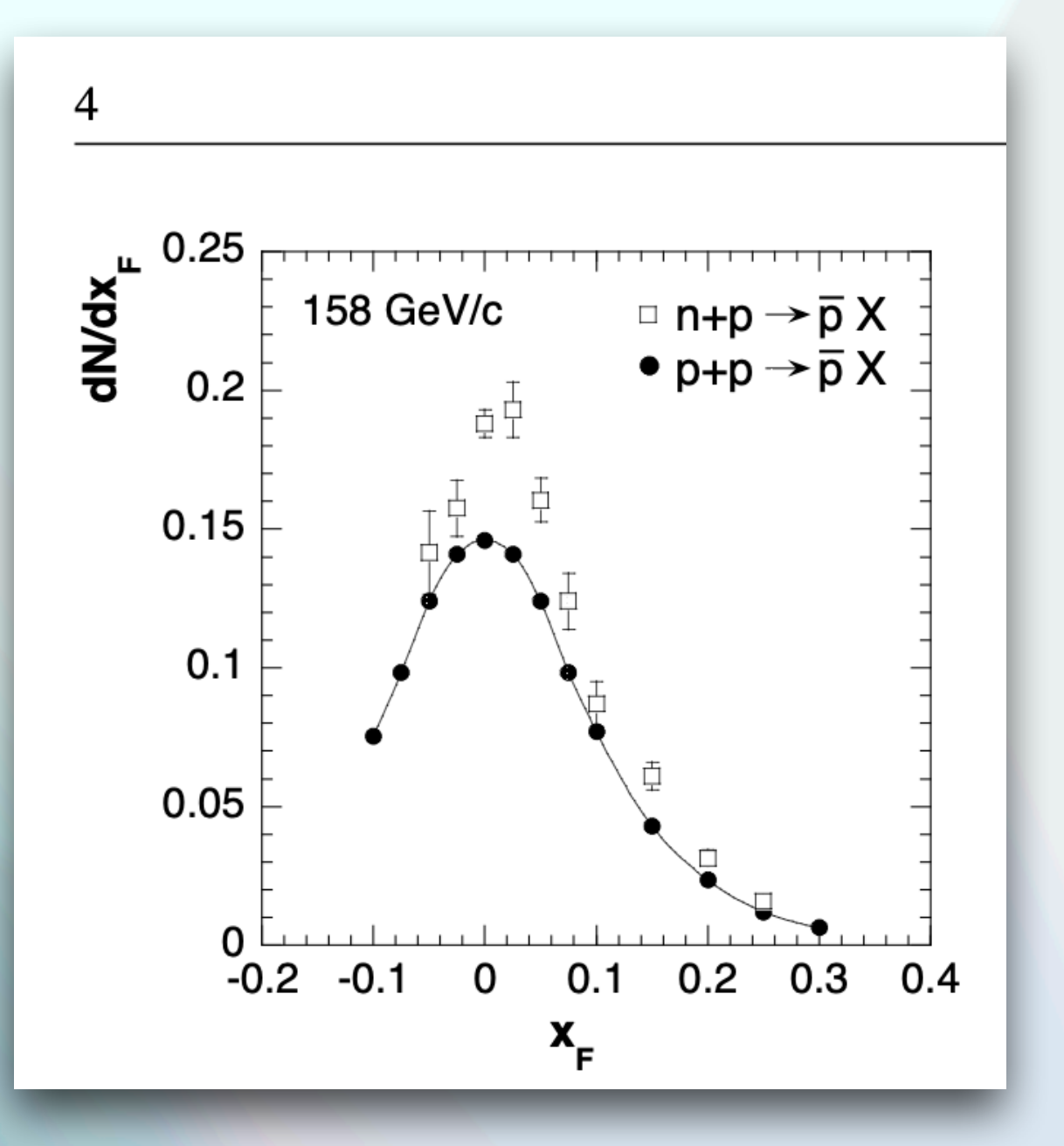
Lorentz-invariant cross section theory curves:



$d\sigma/dx_F$ theory curves:



NA49 2002 data:

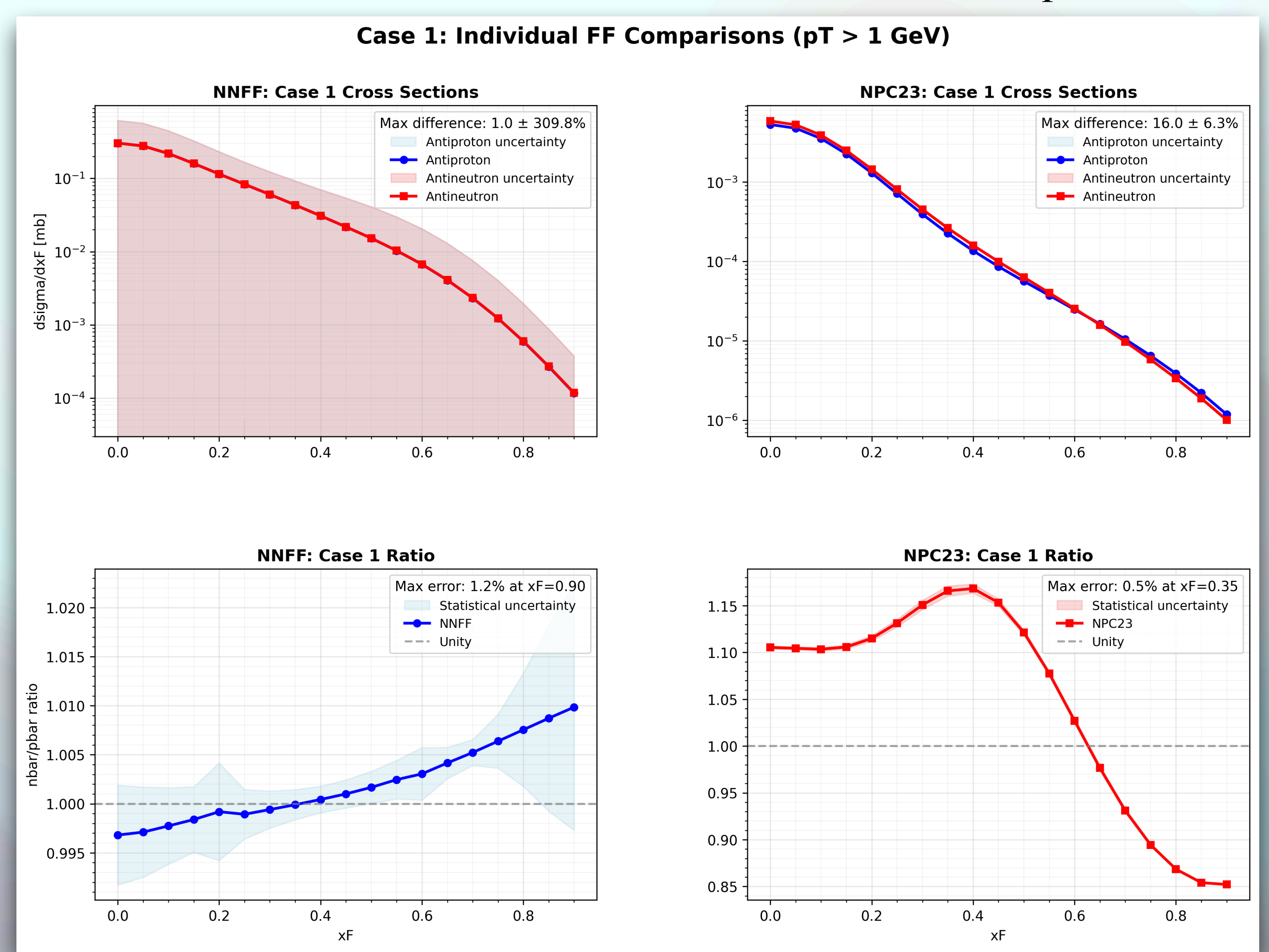


However! Cannot trust theory curves in the low- p_T regime, I integrated from $p_T = 0 - 1$ GeV. Factorization breaks down below 1 GeV.

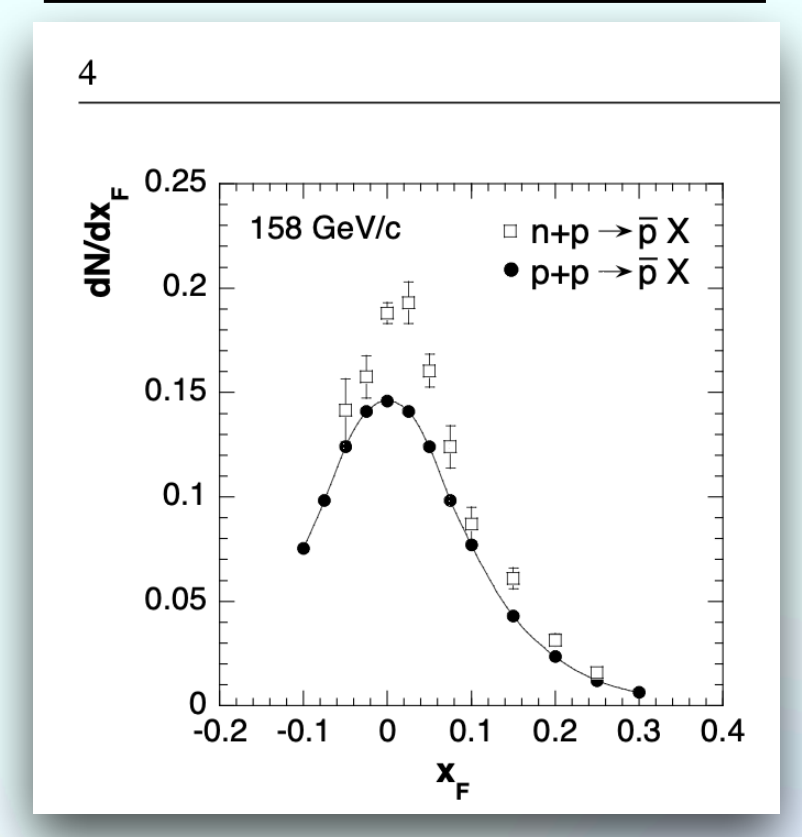
Deal with Low- p_T effects I: Data vs. QCD/Pheno

Calculate using both fragmentation function sets.

NPC23, NNFF theory curves integrated from $p_T \ge 1$ GeV:



NA49 2002 data:



Two investigation paths:

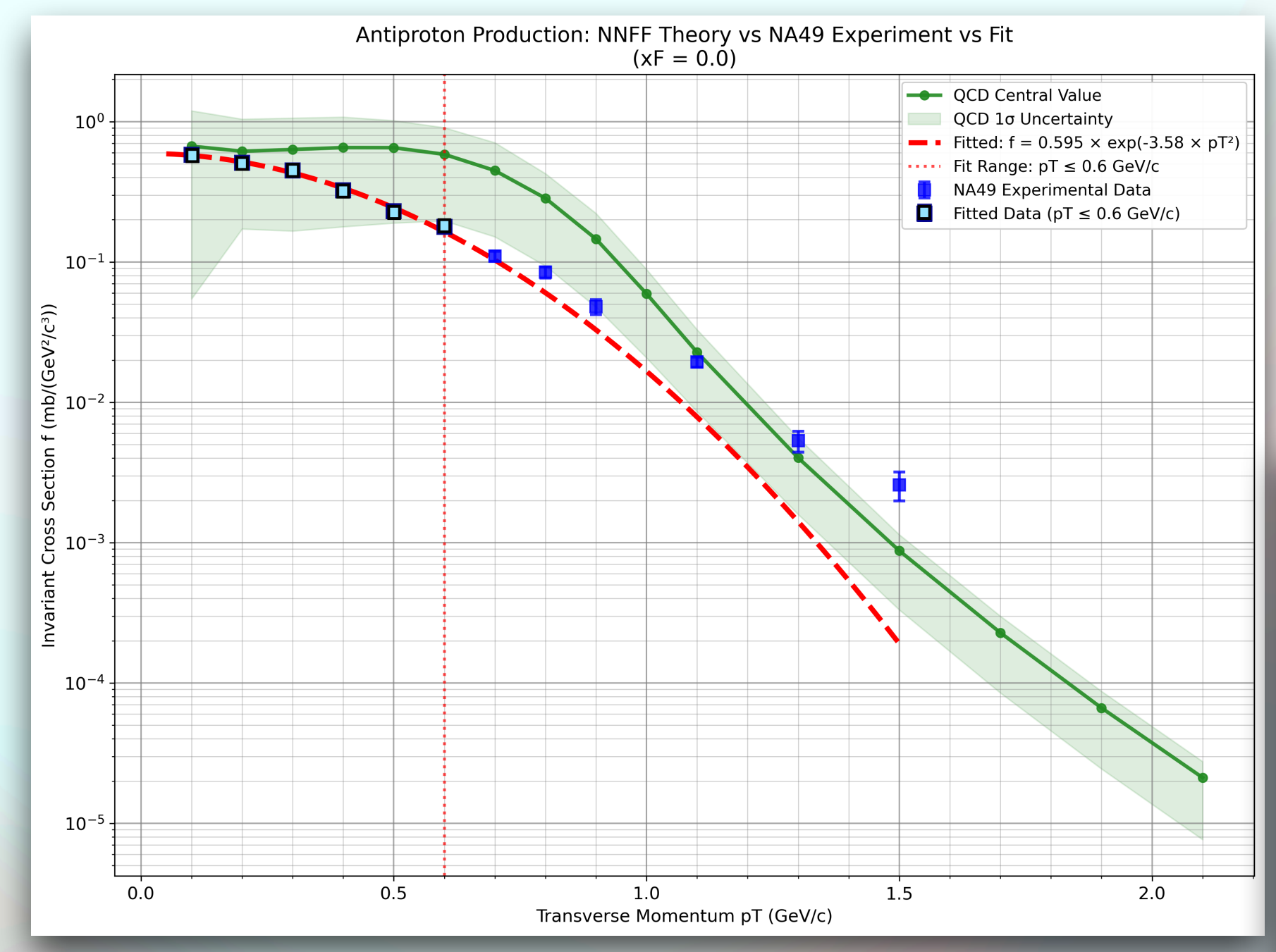
Path 1: Integrate from $p_T = 1 - \infty$

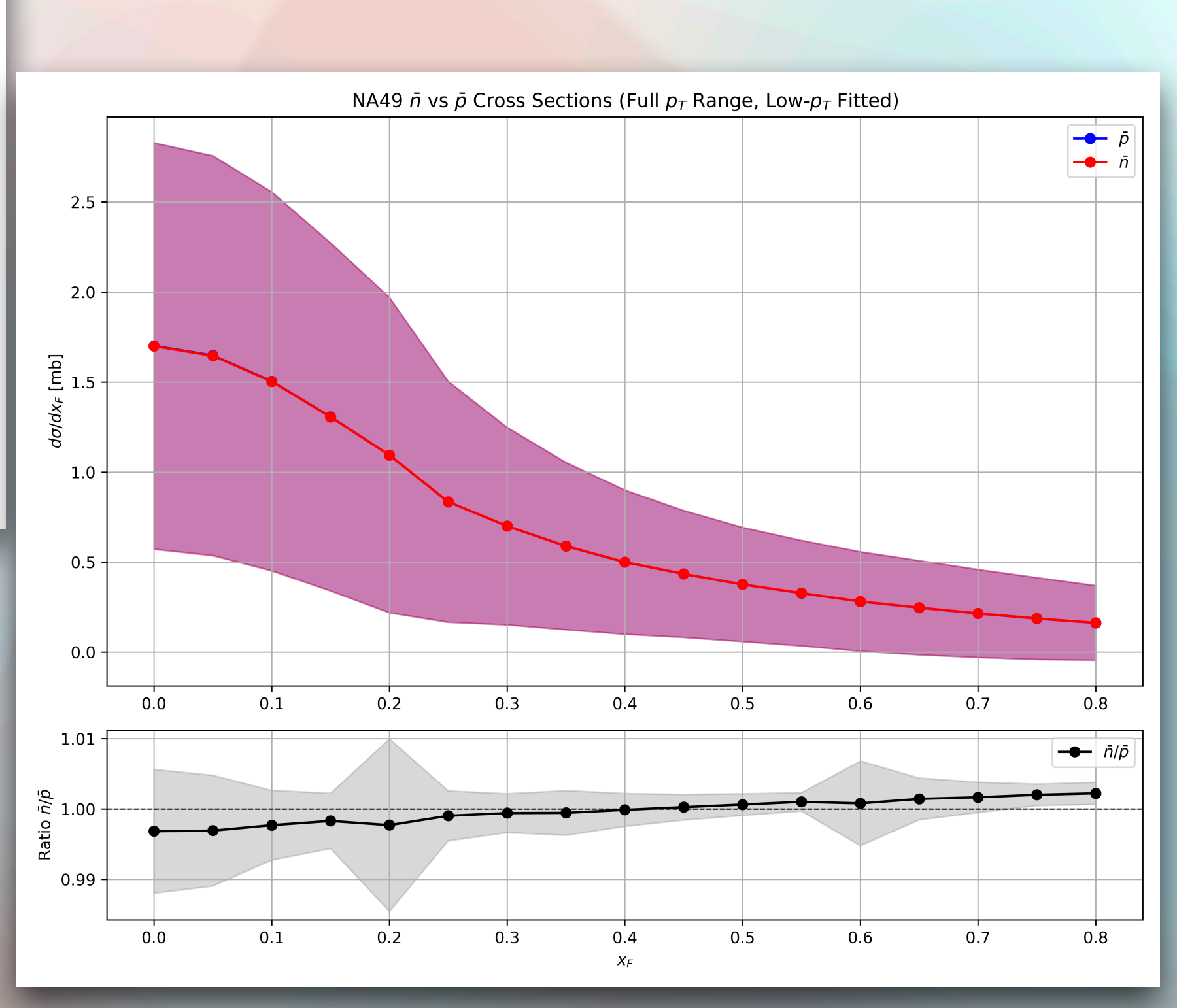
Path 2: Fit low- p_T data, use same fitting function for theory

Deal with Low- p_T effects II: Data vs. QCD/Pheno

Lorentz invariant cross sections vs. p_T :

NNFF theory curves vs. 2010 NA49 data + fitting function:





Two investigation paths:

Path 1: Integrate from $p_T = 1 - \infty$

Path 2: Fit low- p_T data, use same fitting function for theory

Fitting function form from NA49 paper:

$$f = Ae^{-b|t|},$$

with $p_T^2 \sim |t|x_F$

Gluon Fragmentation Functions for $pp \to \bar{N}$

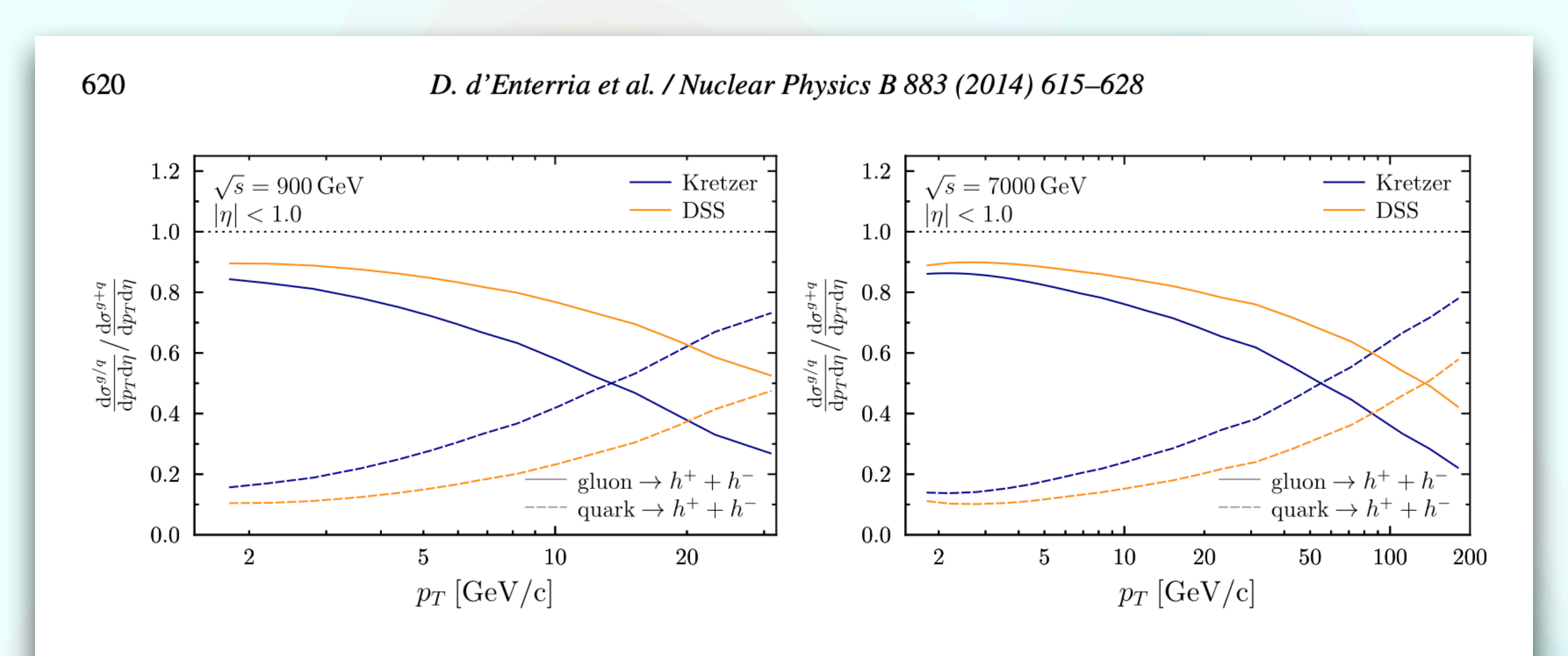


Fig. 3. Relative contributions of quark (dashed) and gluon (solid) fragmentation to the inclusive charged-hadron cross section at $\sqrt{s} = 900$ GeV (left) and $\sqrt{s} = 7000$ GeV (right) at midrapidity, obtained with Kretzer (dark blue) and DSS (orange) FFs. (For interpretation of the references to color in this figure legend, the reader is referred to the web version of this article.)

"Confronting current NLO parton fragmentation functions with inclusive charged-particle spectra at hadron colliders," d'Enterria, Eskola, Helenius & Paukkunen 2014 Nuc.Phys.B

Gluon FFs dominate at low p_T for earlier FFs and NNFF (not NPC23), and gluons are flavor indifferent \therefore we do expect a large difference between \bar{p}, \bar{n}

Calculate Lorentz-invariant NA49 2010 Data vs. QCD/Pheno:

$pp \rightarrow p, pp \rightarrow \bar{p}$

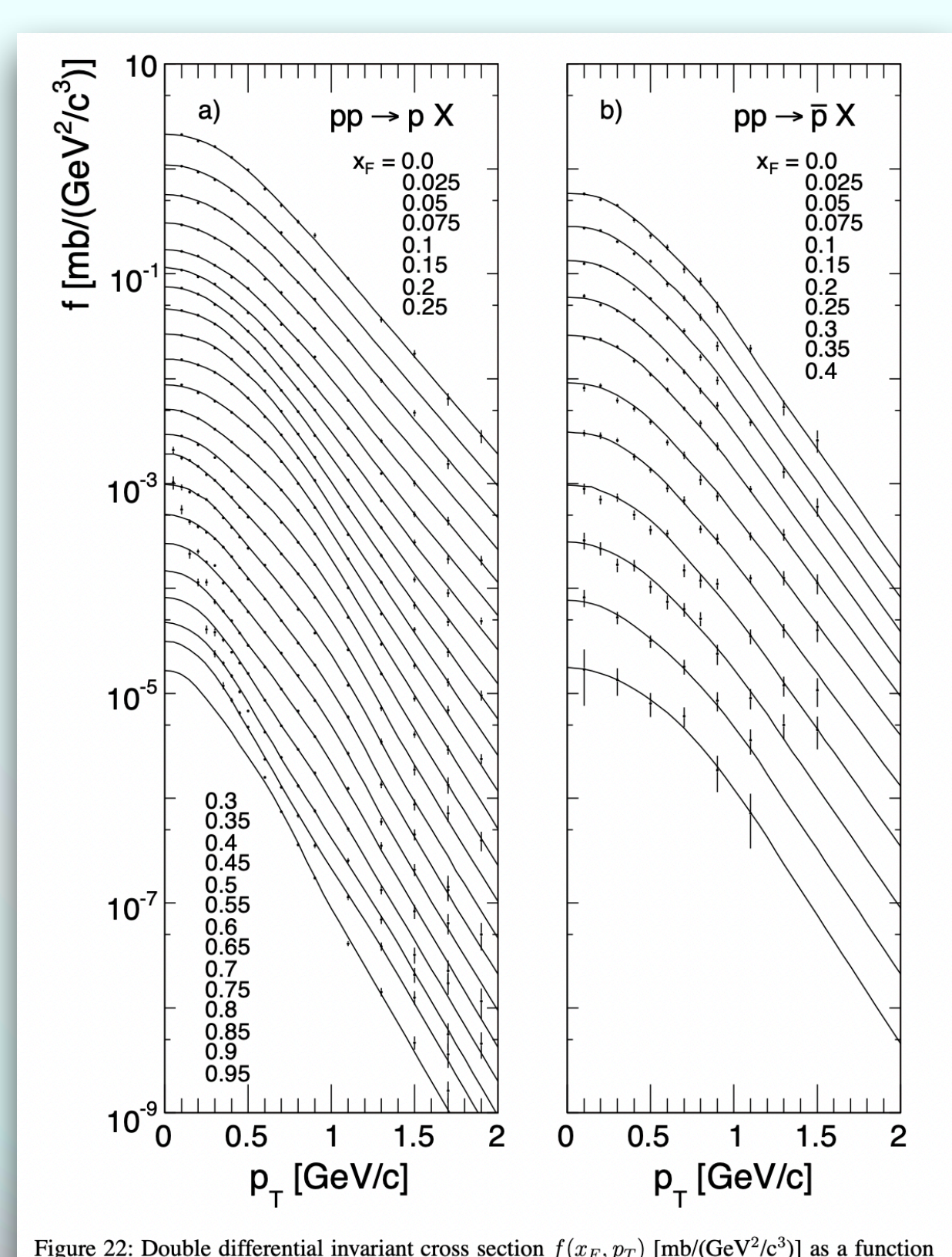
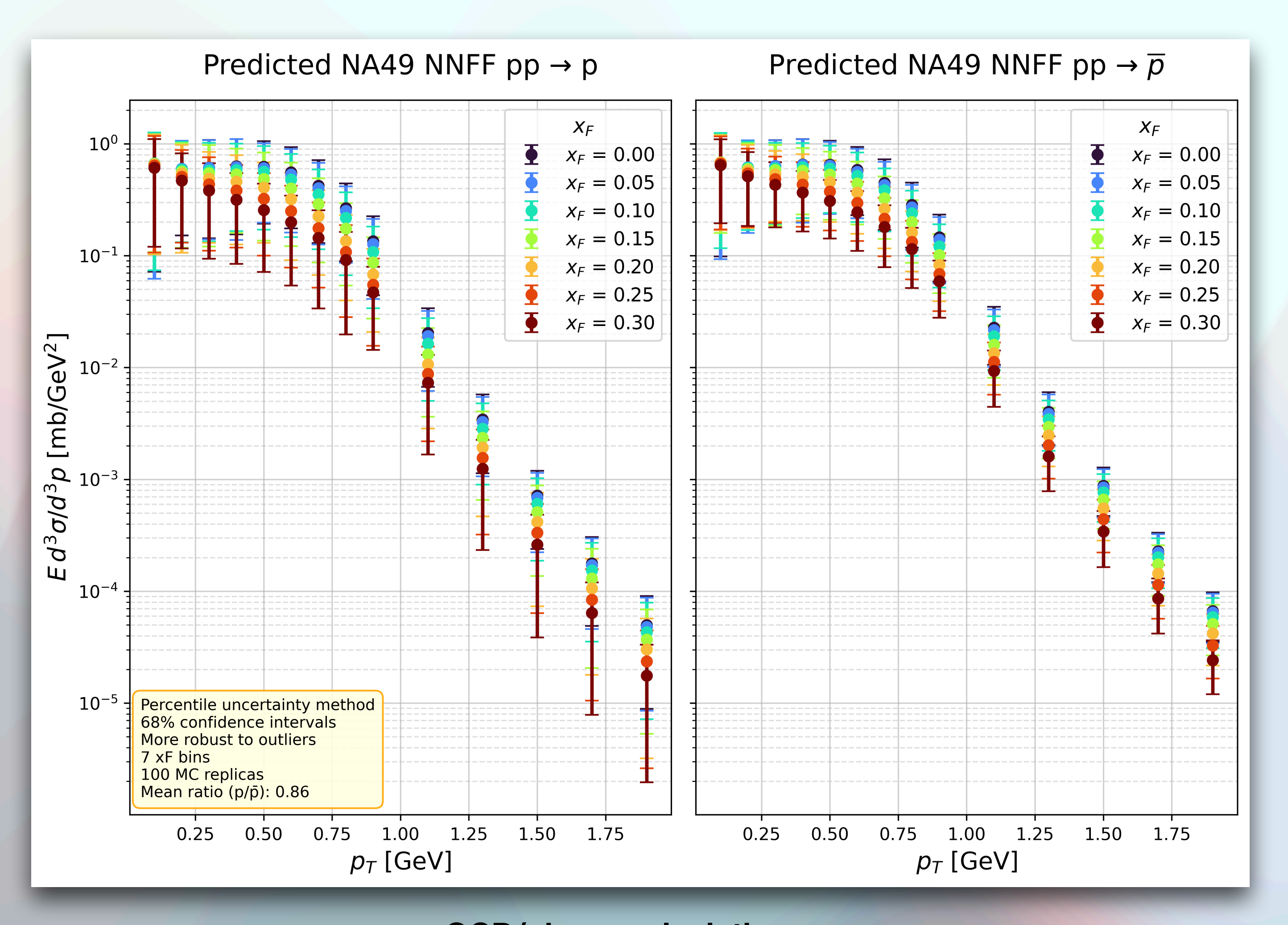


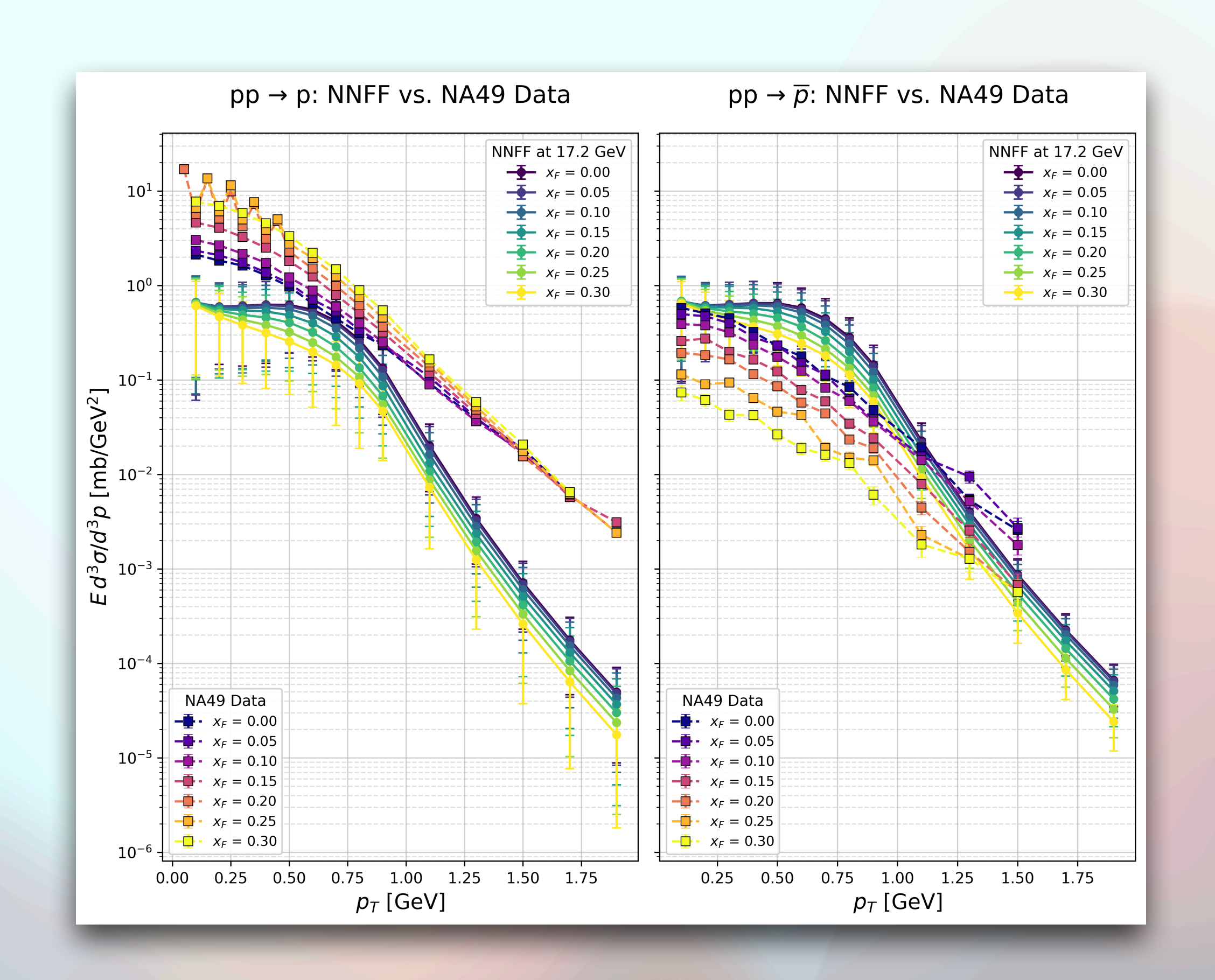
Figure 22: Double differential invariant cross section $f(x_F, p_T)$ [mb/(GeV²/c³)] as a function of p_T at fixed x_F for a) protons and b) anti-protons produced in p+p collisions at 158 GeV/c beam momentum. The distributions for different x_F values are successively scaled down by 0.5 for better separation

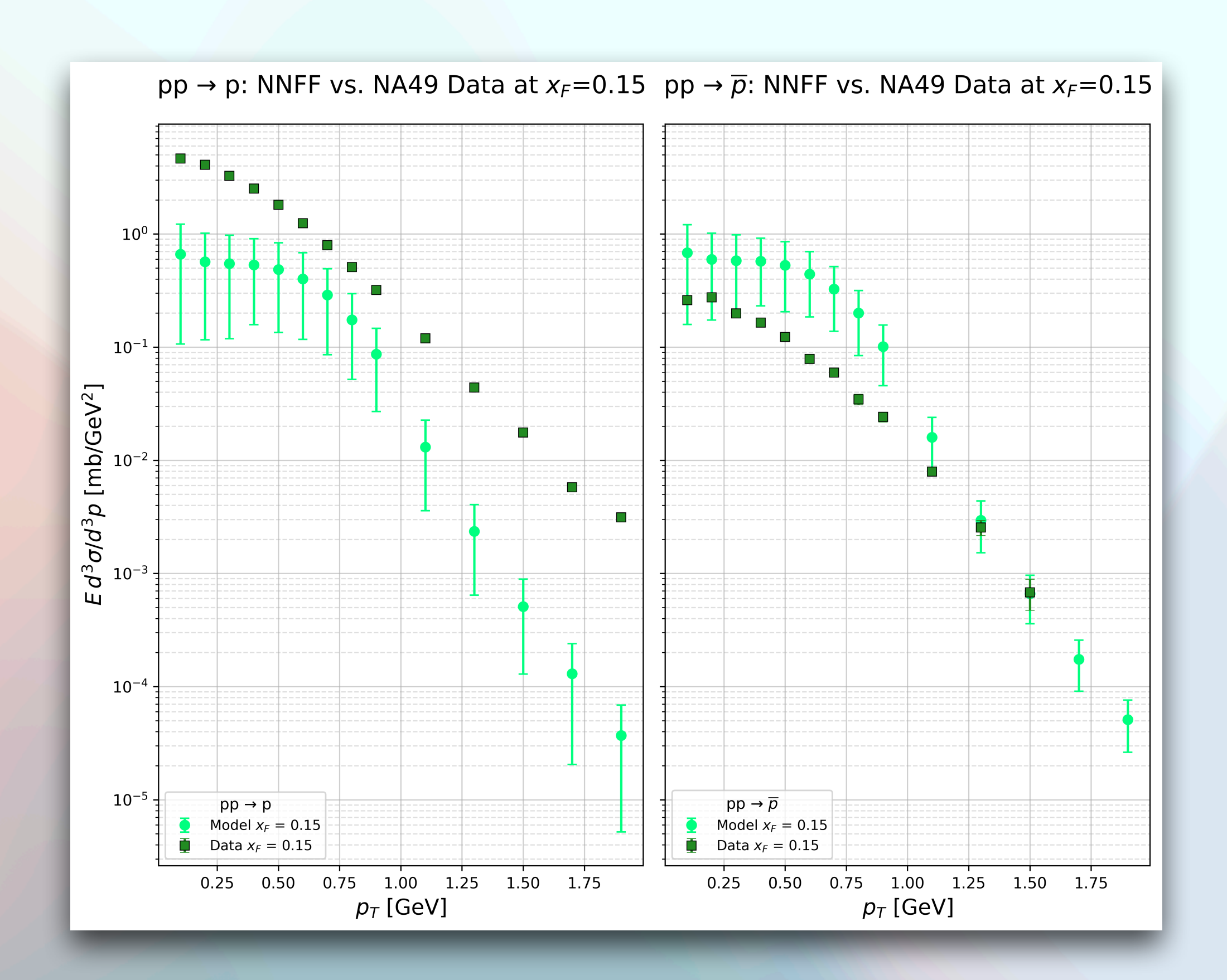
NA49 2010 data...



QCD/pheno calculations...

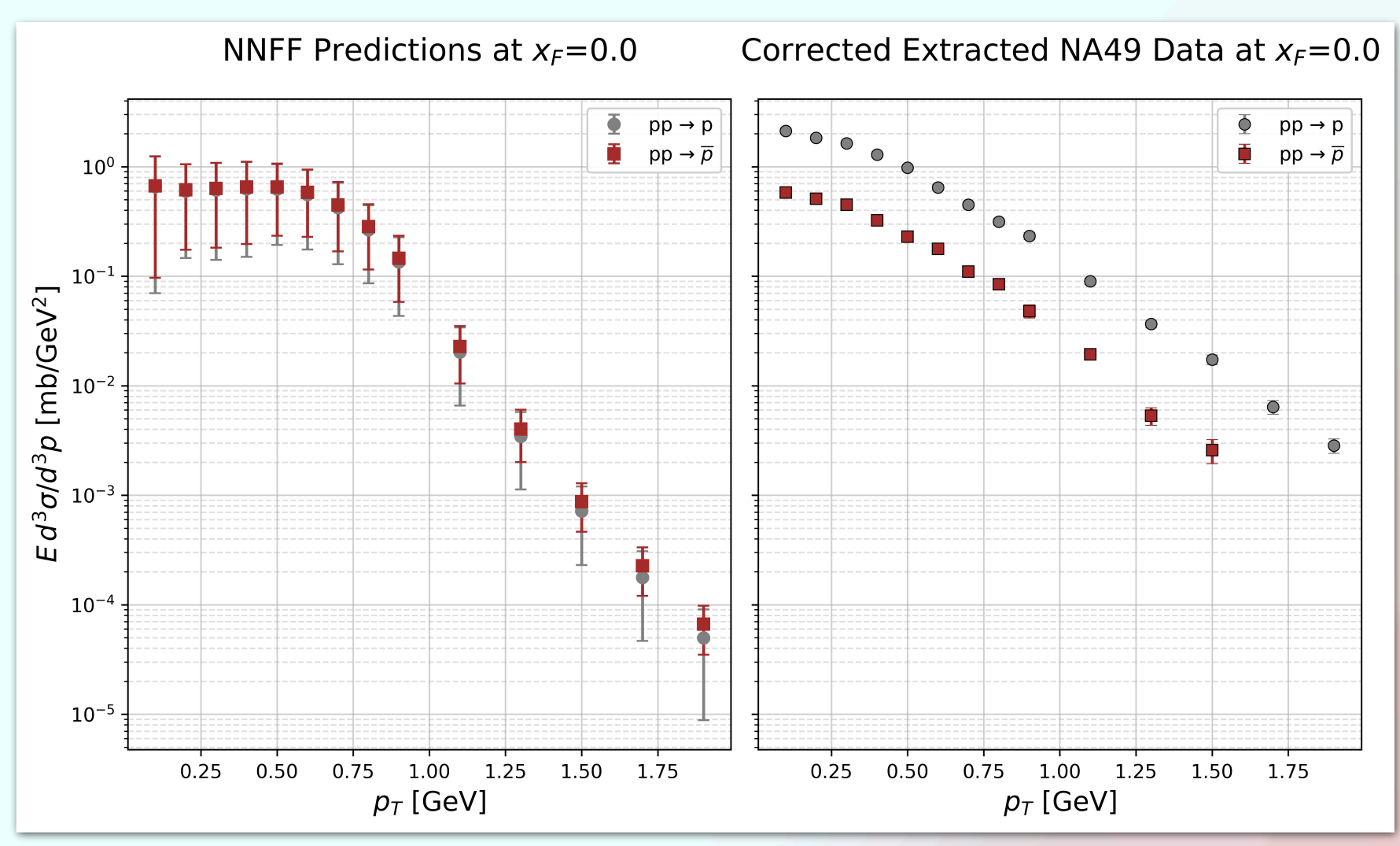
Cross sections for $pp \rightarrow p$, \bar{p}

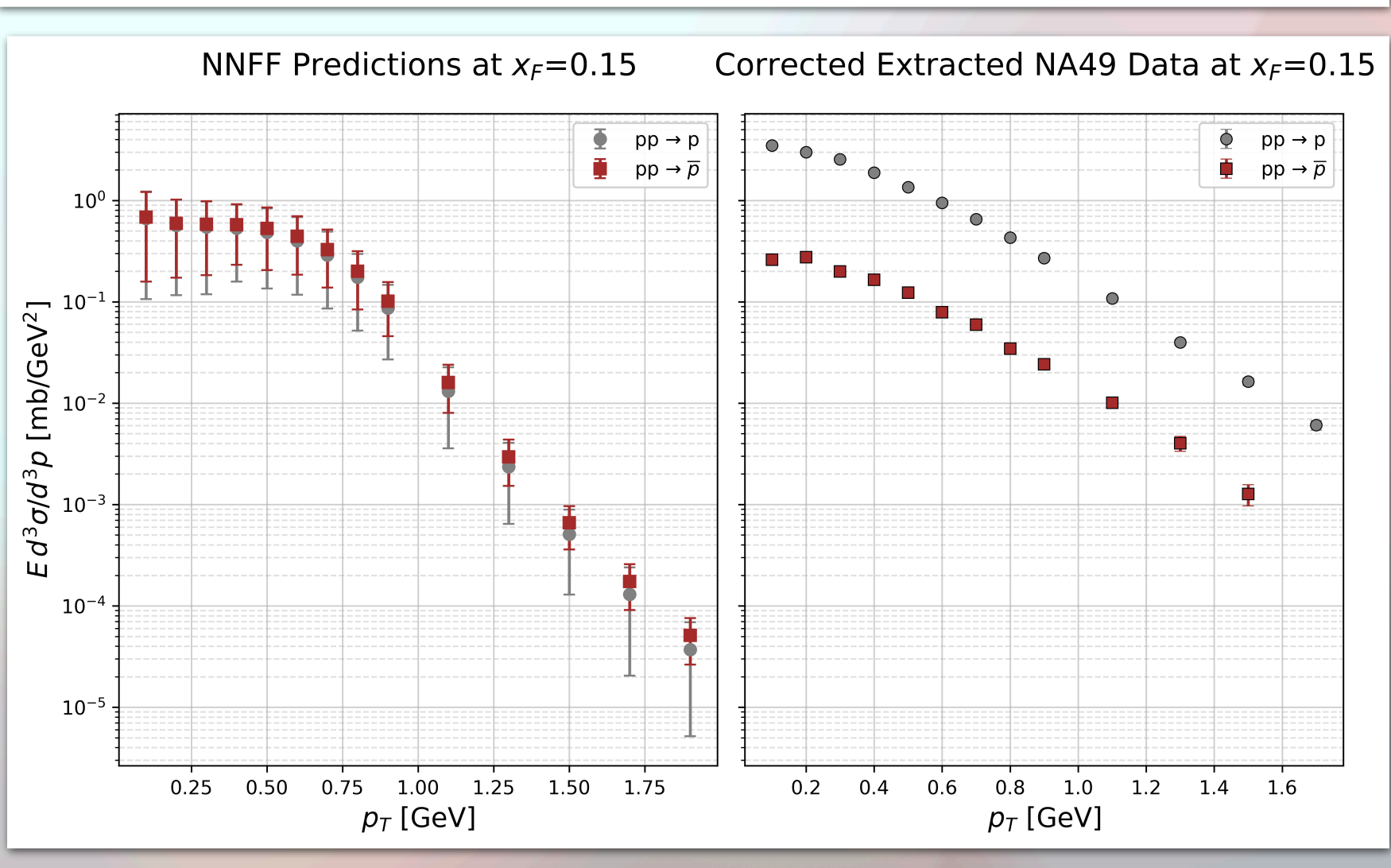


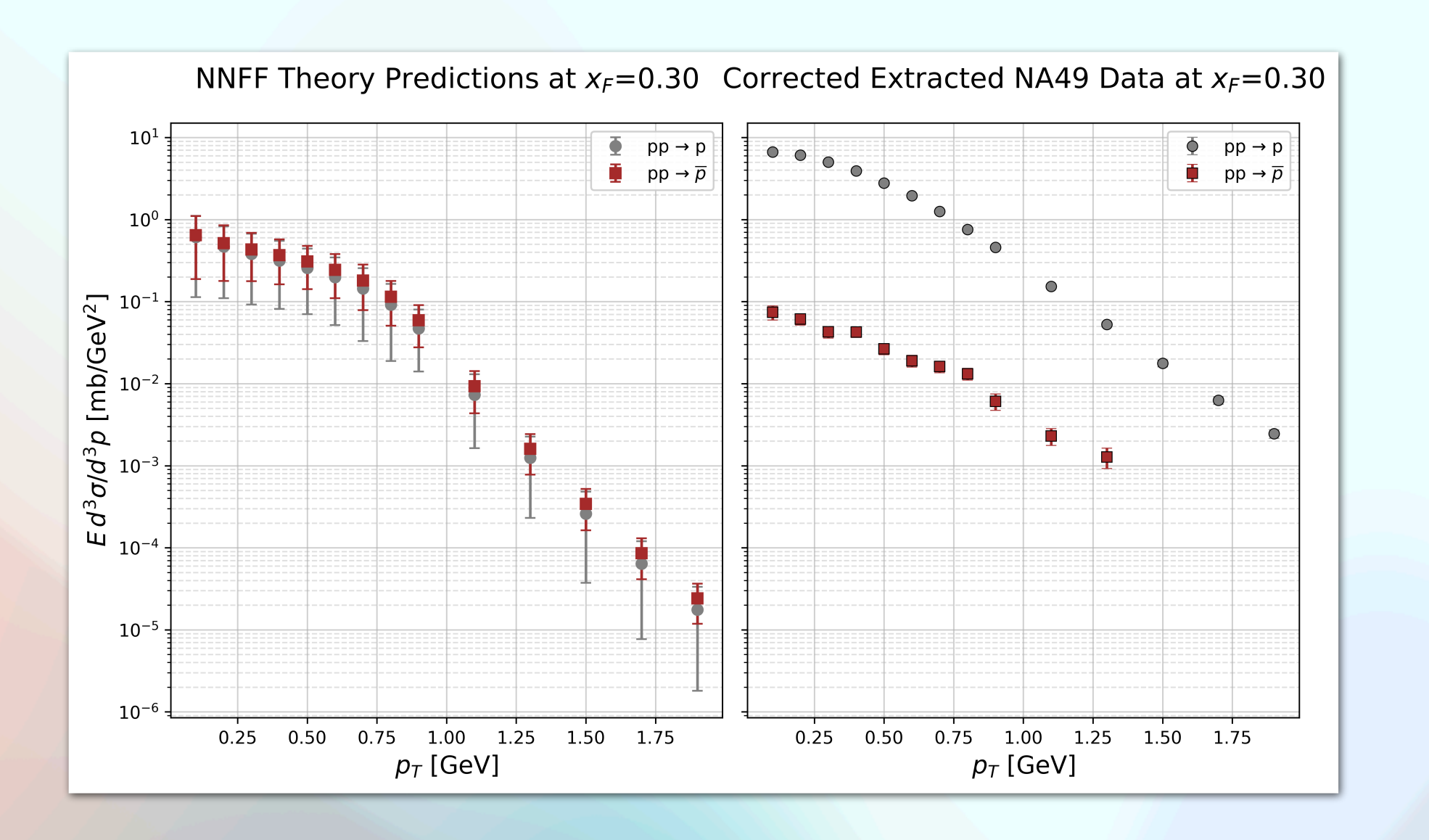


Benchmarking to NA49 2010 data: Proton benchmark failure, antiproton may match within uncertainties

Further analysis of $pp \rightarrow p$, \bar{p}







Conclusions from this analysis:

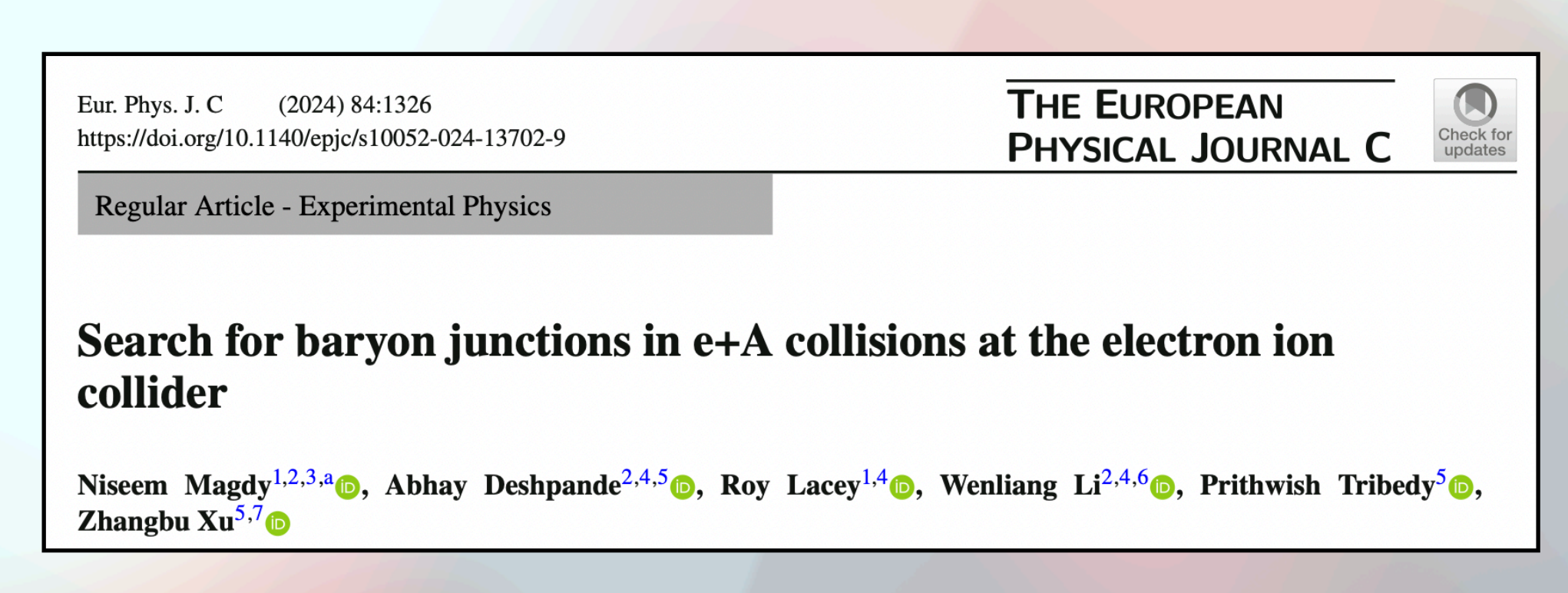
We do not see a 33 % excess in antineutron vs. antiproton production - within error bands, \bar{p} , \bar{n} are identical

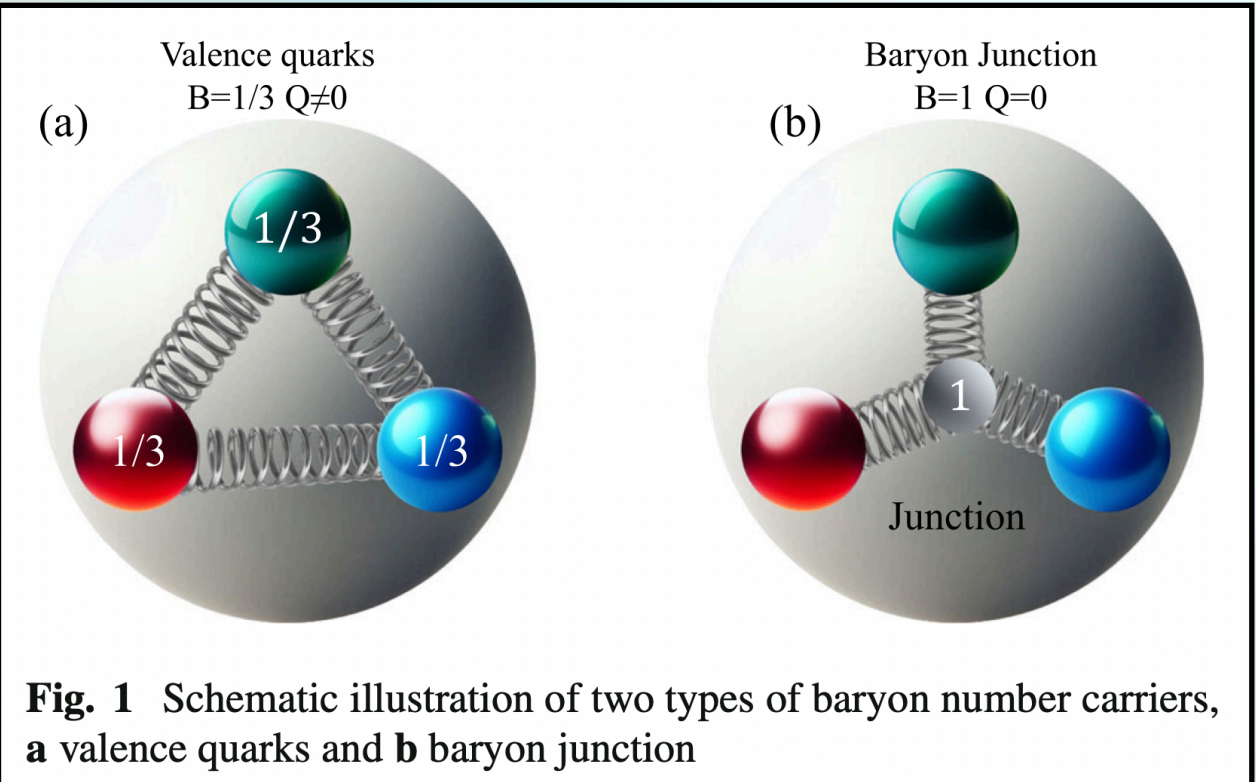
- QCD/pheno cross sections show very slight antiproton increase over proton production, but within errors the same
- NA49 2010 data shows large ratio of $\frac{p}{\bar{p}}$, we do not match their production
- Due to gluon FFs, it seems theory may be correct but, NA61 2017 indicates NA49 2010 was correct in the large p production so this cannot be the whole story...

Global conclusions from these analyses:

- In pp o p vs. pp o ar p at $\sqrt{s} = 17.2$ GeV, a discrepancy between data and theory exists
- Either our QCD/pheno calculations have problems, or
- NA49/NA61 (also AGS and others) data have problems, or
- Both of the above, or
- Neither of the above, in which case nonperturbative effects may be coming into play

This last choice has been studied since at least 1996, via Kharzeev's gluon junction model





My followup work:

QCD contributions exist, beyond our calculations, in the form of Active Diquarks

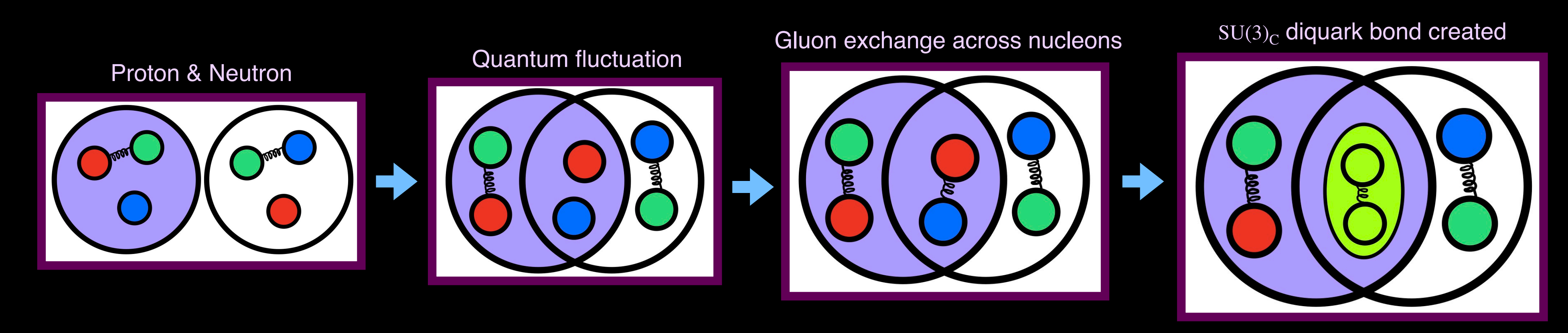
aka Diquark Knockout

aka Diquark Transport of Baryon Number

2021-2023 Diquark work:

Short-range correlations: Fundamental QCD dynamics in NN

Schematic: Diquark formation as cause of short-range correlations (SRC), modifying quark behavior in the NN pair



Color scheme: The 3 SU(3) color charges are the usual red, green, blue - anticolor charge of antigreen represented by lime green

3N SRC a work in progress, diquark-based SRC makes predictions. 4N is published, the hidden color hexadiquark state...

JRW, S.J.Brodsky, G. de Teramond, I.Schmidt, A.Goldhaber, arXiv:2004.14659, Nuc. Phys A 2021

2023 Diquark work:

Diquark binding energy from Color hyperfine structure

Use Λ^0 baryon to find binding energy of [ud]:

B.E.
$$[ud] = m_u^b + m_d^b + m_s^b - M_{\Lambda^0}$$

Spin-spin interaction contributes to hadron mass; QCD hyperfine interactions:

1.
$$M_{\text{(baryon)}} = \sum_{i=1}^{3} m_i + a' \sum_{i < j} \left(\sigma_i \cdot \sigma_j \right) / m_i m_j$$

2.
$$M_{\text{(meson)}} = m_1 + m_2 + a \left(\sigma_1 \cdot \sigma_2\right) / m_1 m_2$$

(de Rujula, Georgi & Glashow 1975, Gasiorowicz & Rosner 1981, Karliner & Rosner 2014)

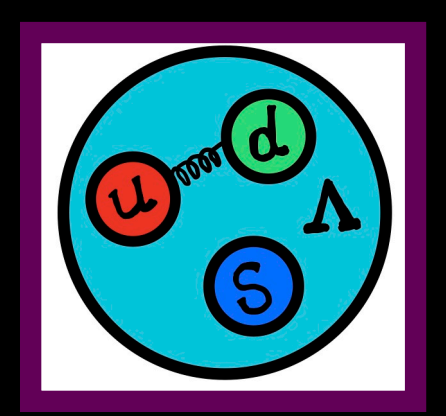
Effective masses of light quarks are found using Eq.1 and fitting to measured baryon masses:

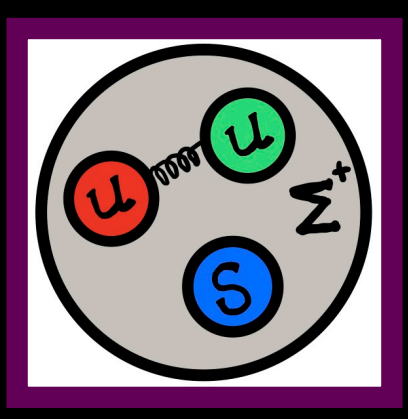
$$m_u^b = m_d^b \equiv m_q^b = 363 \text{ MeV}, \ m_s^b = 538 \text{ MeV}$$

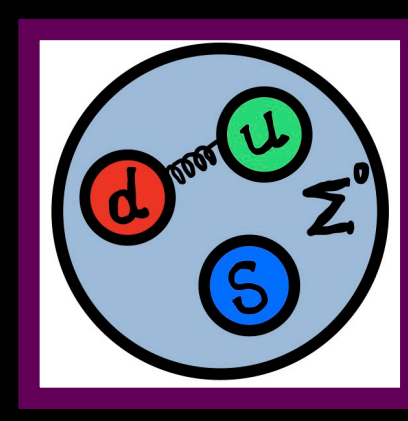
B.E._[ud] =
$$m_u^b + m_d^b + m_s^b - M_{\Lambda} = 148 \pm 9 \text{ MeV}$$

[NB: Diquark-carrying baryons Λ_c , Σ_c^+ , Σ_c^0 , $\Sigma_c^- \Longrightarrow \sim 159 \pm 10 \text{ MeV}$]

Relevant diquark-carrying baryons: Λ , Σ^+ , Σ^0 , Σ^-







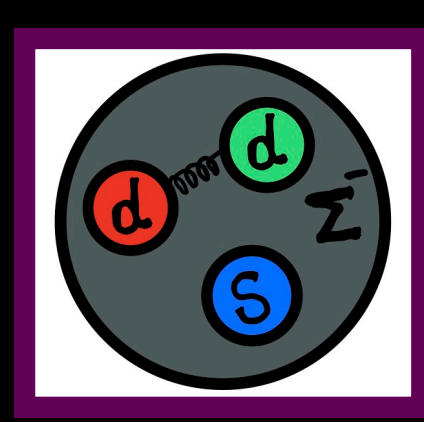


TABLE I: Diquark properties

Diquark B	inding Energy (Me	V) Mass (MeV)	Isospir	n I Spin S
[ud]	148 ± 9	\mid 578 \pm 11 \mid	0	0
(ud)	0	$ 776 \pm 11 $	1	1
(uu)	0	776 ± 11	1	1
(dd)	0	776 ± 11	1	1

Uncertainties calculated using average light quark mass errors $\Delta m_q = 5~MeV~[37]$

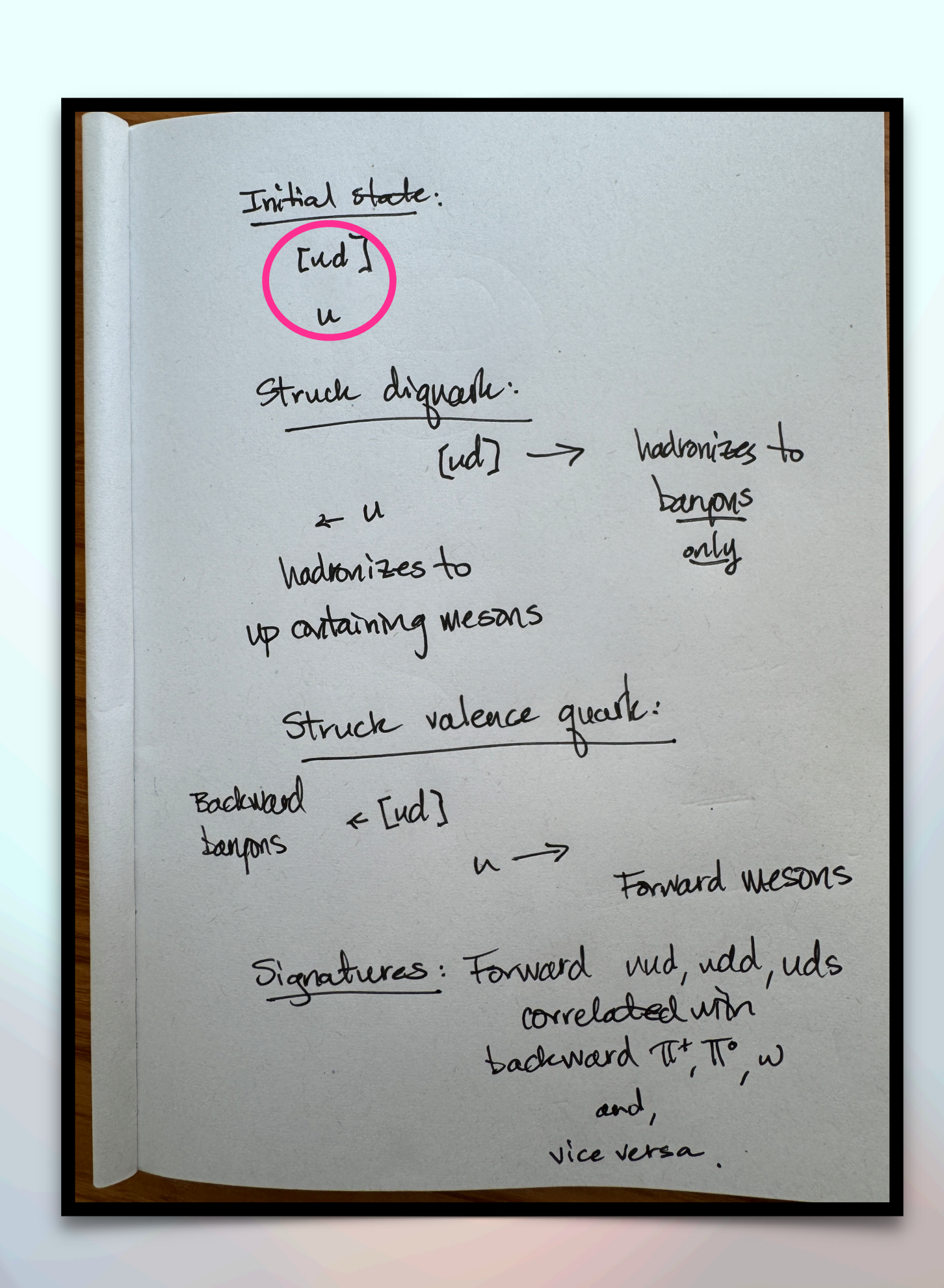
TABLE II: Relevant SU(3)_C hyperfine structure baryons [28]

Λ	[ud]s	1115.683 ± 0.006	$3 \left 0 \left(\frac{1}{2} \right) \right $	
Σ^+	(uu)s	1189.37 ± 0.07	$1\left(\frac{1}{2}^+\right)$	
Σ^0	(ud)s	1192.642 ± 0.024	$\left 1\left(\frac{1}{2}\right)\right $	
Σ^-	(dd)s	$ 1197.449 \pm 0.030$	$0 \left 1 \left(\frac{1}{2} \right) \right $	

 $I\left(J^{P}
ight)$ denotes the usual isospin I, total spin J and parity P quantum numbers, all have $L\!=\!0$ therefore J=S

"Diquark Induced Short-Range Correlations & the EMC Effect," JRW, Nucl.Phys.A 2023

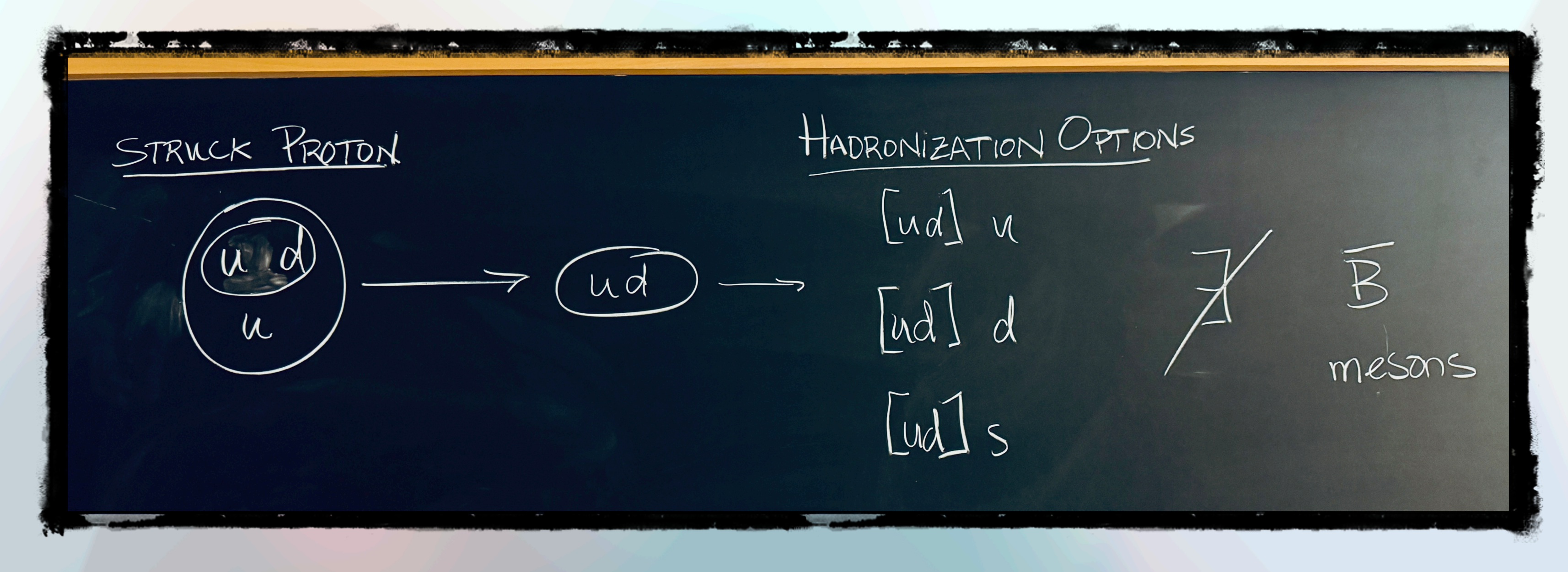
Diquark transport/knockout model



SIGNATURES:

Forward baryons, backward light-quark carrying mesons - no J/ψ with its $c\bar{c}!$

Forward light quark carrying mesons, backward baryons



Two draft manuscripts in progress:

"Diquark Knockout Model for Backward-Angle Meson Production in u-Channel Scattering"

& "Diquark Transport of Baryon Number"

To be posted...grazie!

Jennifer Rittenhouse West
INFN Section Turin & Physics Department, University of Turin

XX Conference on Theoretical Nuclear Physics in Italy II Palazzone di Cortona 1-3 October 2025

Cortona, Italia



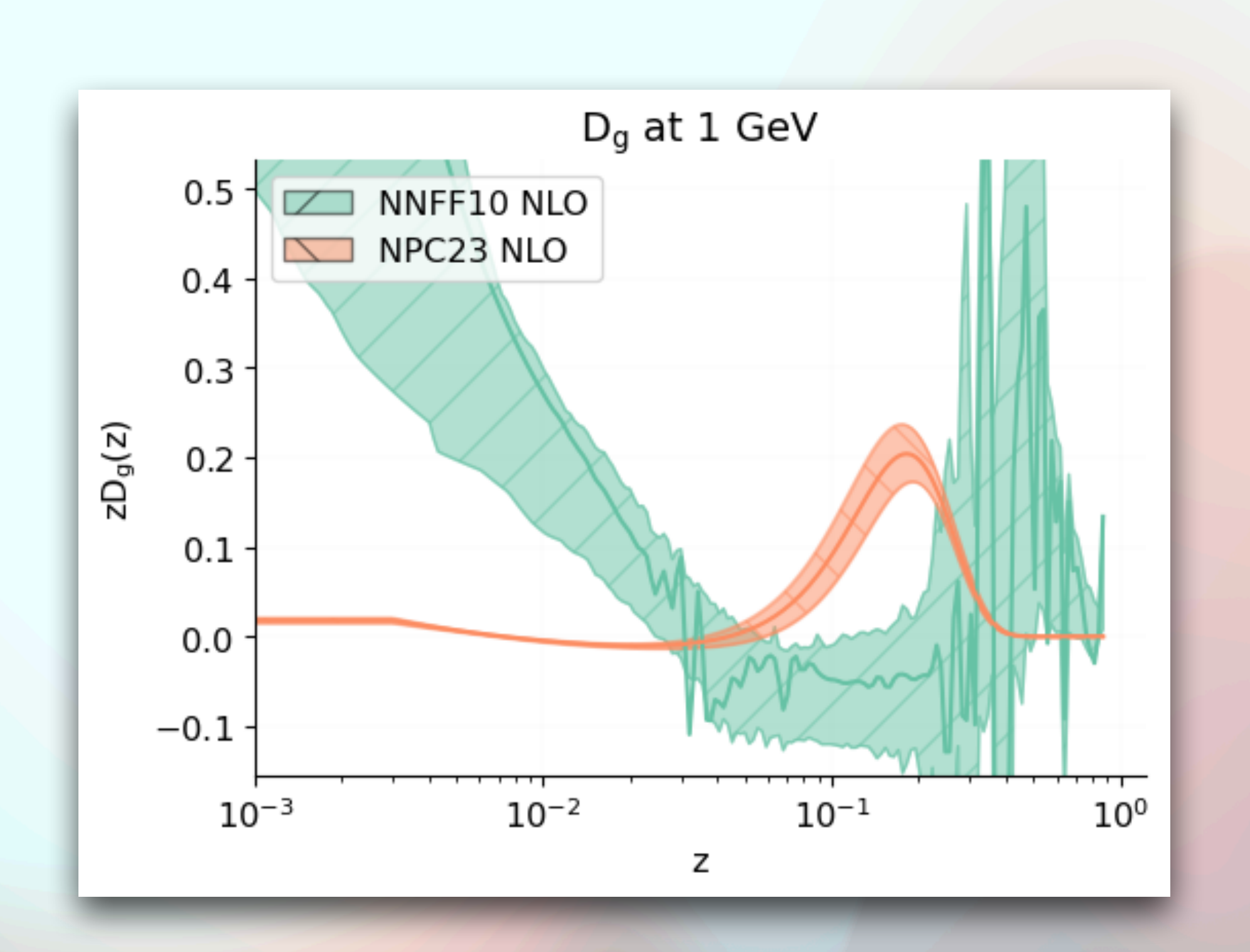
EIC2
EIC Center at Jefferson Lab

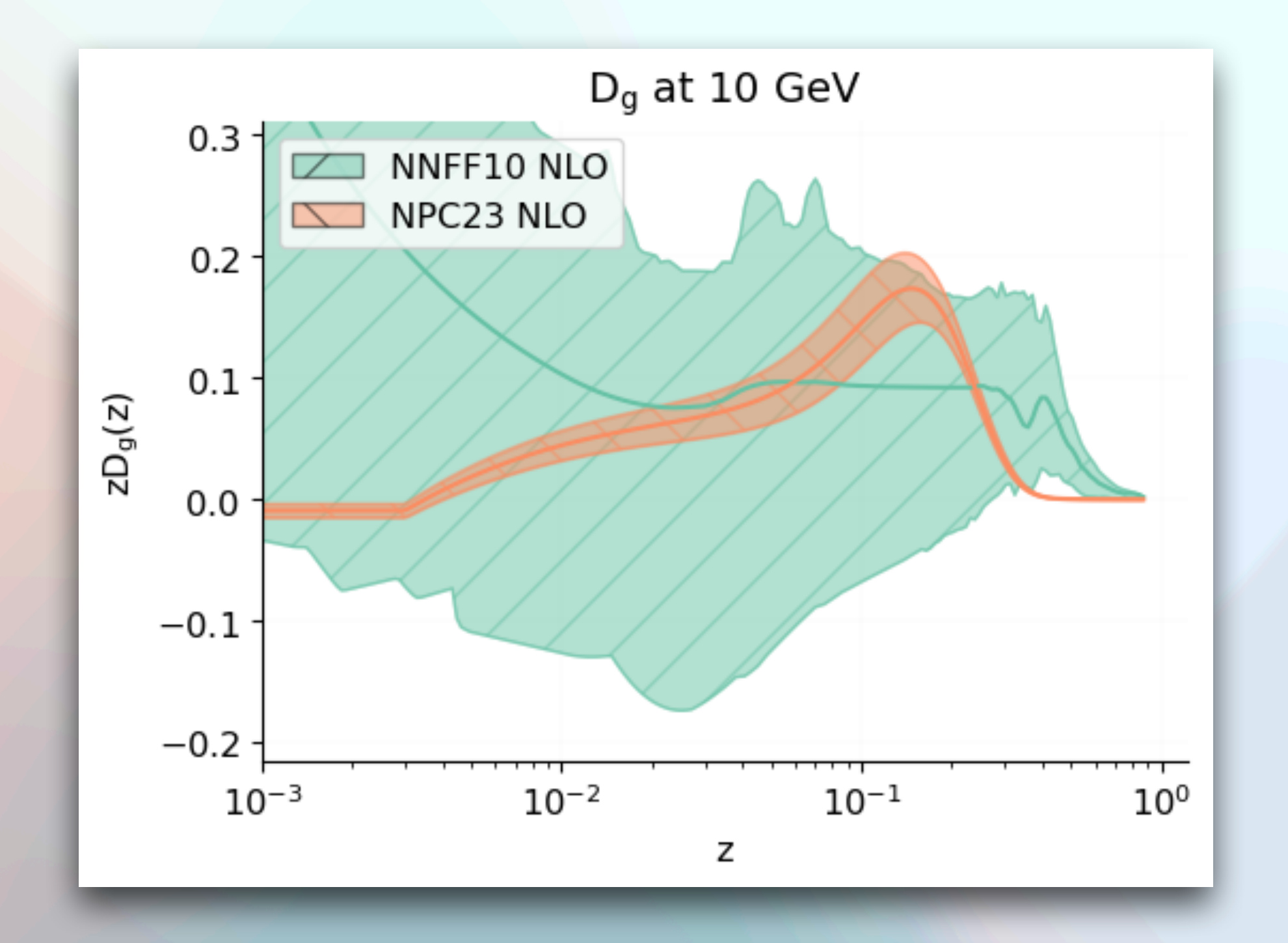
Berkeley
UNIVERSITY OF CALIFORNIA



Gluon \bar{p} Fragmentation Function Comparisons

 $g
ightarrow \bar{p}$ FF at 1 GeV & 10 GeV

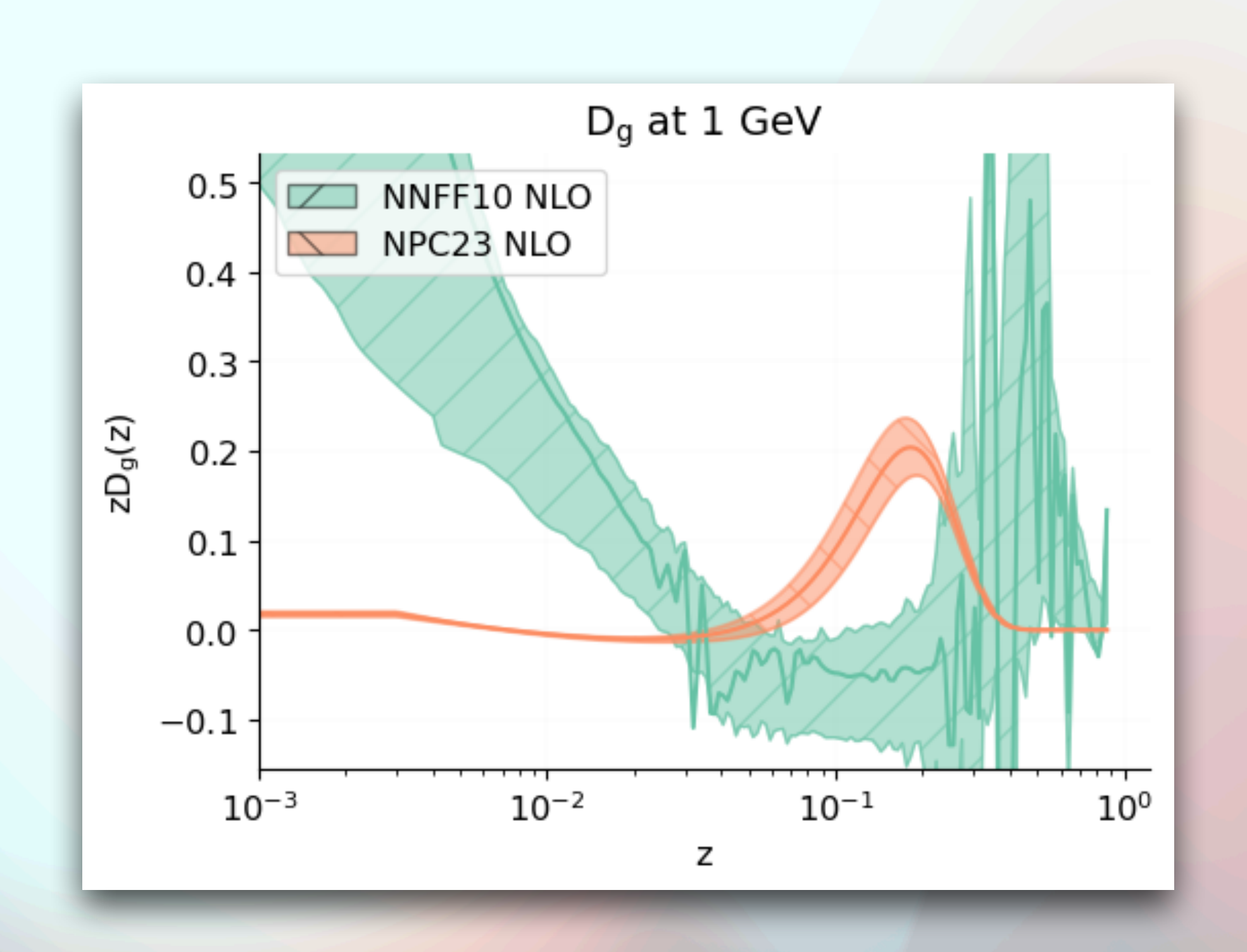


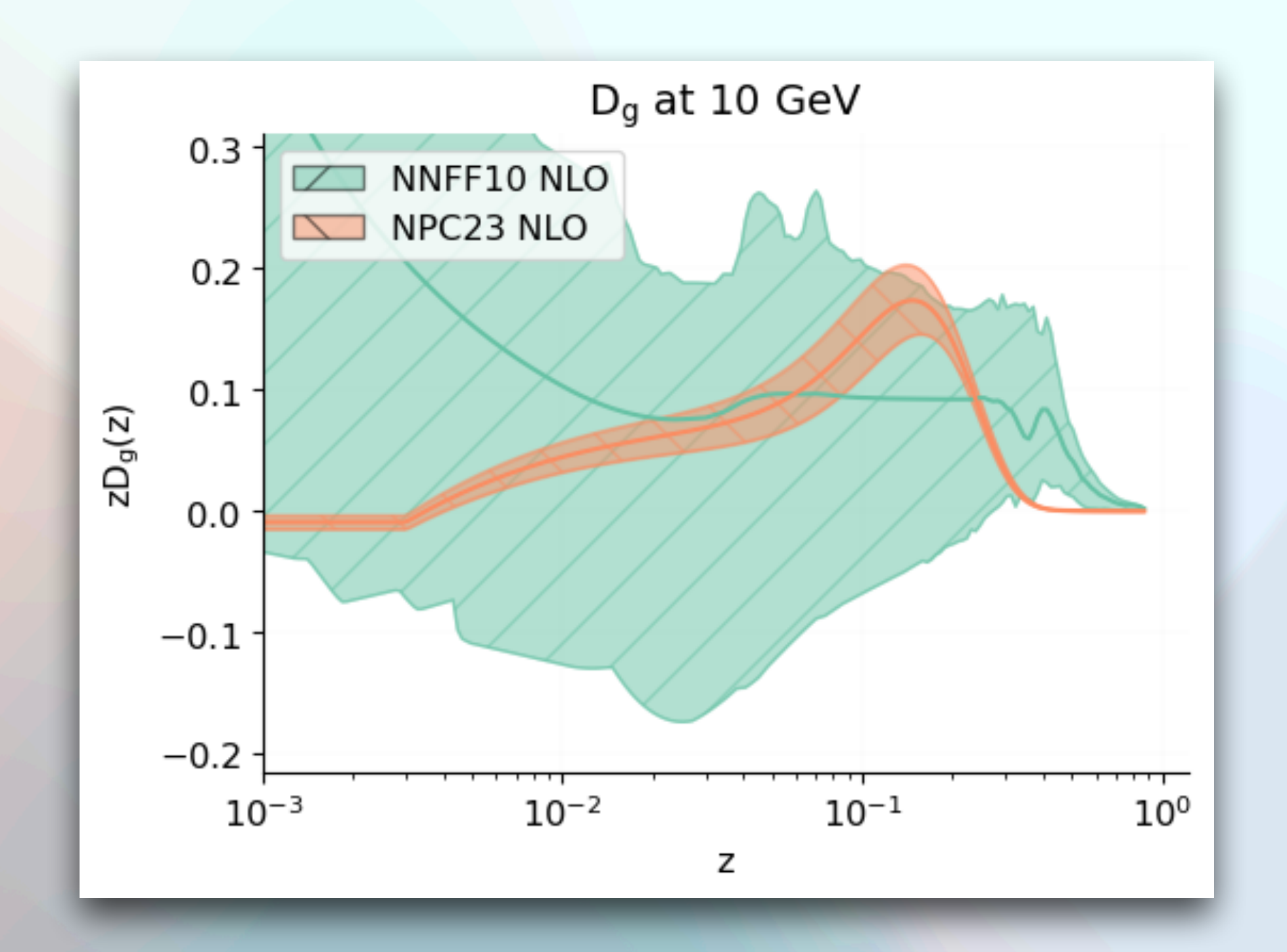


Gluon FFs dominate at low p_T , NNFF error bands become larger as p_T increases

Gluon \bar{n} Fragmentation Function Comparisons

 $g \rightarrow \bar{n}$ FFs at 1 GeV & 10 GeV





Gluon FFs may dominate at low p_T , error bands become larger as p_T increases